2mic

NASA TECHNICAL NOTE

NASA TN D-7667

NASA TN D-7667



# SOUND RADIATION FROM A HIGH-SPEED AXIAL-FLOW FAN DUE TO THE INLET TURBULENCE QUADRUPOLE INTERACTION

*by Marvin E. Goldstein, Burt M. Rosenbaum, and Lynn U. Albers*

*Lewis Research Center*
*Cleveland, Ohio 44135*

NATIONAL AERONAUTICS AND SPACE ADMINISTRATION • WASHINGTON, D. C. • JUNE 1974

| 1. Report No. NASA TN D-7667 | 2. Government Accession No. | 3. Recipient's Catalog No. |
|---|---|---|
| 4. Title and Subtitle SOUND RADIATION FROM A HIGH-SPEED AXIAL-FLOW FAN DUE TO THE INLET TURBULENCE QUADRUPOLE INTERACTION | | 5. Report Date JUNE 1974<br>6. Performing Organization Code |
| 7. Author(s) Marvin E. Goldstein, Burt M. Rosenbaum, and Lynn U. Albers | | 8. Performing Organization Report No. E-7741<br>10. Work Unit No. 501-04 |
| 9. Performing Organization Name and Address Lewis Research Center, National Aeronautics and Space Administration, Cleveland, Ohio 44135 | | 11. Contract or Grant No.<br>13. Type of Report and Period Covered Technical Note |
| 12. Sponsoring Agency Name and Address National Aeronautics and Space Administration, Washington, D.C. 20546 | | 14. Sponsoring Agency Code |

15. Supplementary Notes

16. Abstract

One of the dominant sources of broadband noise (and possibly also of pure tones) in aircraft engine fans is the turbulence drawn into the fan inlet. A number of investigations have analyzed this noise source by using a dipole model. However, at the high subsonic Mach numbers at which some current engine fans operate, the quadrupole mechanism may be dominant over the dipole mechanism. In such a case, analyses based on the dipole model are unsatisfactory. No analysis of this noise source which is based on the quadrupole model and is suitable for high subsonic Mach numbers has been given. The present report is written to fill this gap. A formula is obtained for the total acoustic power spectra radiated out the front of the fan as a function of frequency. The formula involves the design parameters of the fan as well as the statistical properties of the incident turbulence. Numerical results are calculated for values of the parameters in the range of interest for quiet fans tested at the Lewis Research Center. As in the dipole analysis, when the turbulence correlation lengths become equal to the interblade spacing, the predicted spectra exhibit peaks around the blade passing frequency and its harmonics. There has recently been considerable conjecture about whether the stretching of turbulent eddies as they enter a stationary fan could result in the inlet turbulence being the dominant source of pure tones from nontranslating fans (i.e., fans in nonmoving aircraft). The results of the current analysis show that, unless the turbulent eddies become quite elongated, this noise source contributes predominantly to the broadband spectrum.

17. Key Words (Suggested by Author(s))
Fan noise
Acoustics
Aerodynamic sound

18. Distribution Statement
Unclassified - unlimited
Category - 01

| 19. Security Classif. (of this report) | 20. Security Classif. (of this page) | 21. No. of Pages | 22. Price* |
|---|---|---|---|
| Unclassified | Unclassified | 47 | $3.25 |

* For sale by the National Technical Information Service, Springfield, Virginia 22151

# SOUND RADIATION FROM A HIGH-SPEED AXIAL-FLOW FAN DUE TO THE INLET TURBULENCE QUADRUPOLE INTERACTION

by Marvin E. Goldstein, Burt M. Rosenbaum, and Lynn U. Albers

Lewis Research Center

## SUMMARY

One of the dominant sources of broadband noise (and possibly also of pure tones) in aircraft engine fans is the turbulence drawn into the fan inlet. A number of investigations have analyzed this noise source by using a dipole model. However, at the high subsonic Mach numbers at which some current engine fans operate, the quadrupole mechanism may be dominant over the dipole mechanism. In such a case, analyses based on the dipole model are unsatisfactory. No analysis of this noise source which is based on the quadrupole model and is suitable for high subsonic Mach numbers has been given. The present report is written to fill this gap.

A formula is obtained for the total acoustic power spectra radiated out the front of the fan as a function of frequency. The formula involves the design parameters of the fan as well as the statistical properties of the incident turbulence. Numerical results are calculated for values of the parameters in the range of interest for quiet fans tested at the Lewis Research Center. As in the dipole analysis, when the turbulence correlation lengths become equal to the interblade spacing, the predicted spectra exhibit peaks around the blade passing frequency and its harmonics. There has recently been considerable conjecture about whether the stretching of turbulent eddies as they enter a stationary fan could result in the inlet turbulence being the dominant source of pure tones from nontranslating fans (i. e., fans in nonmoving aircraft). The results of the current analysis show that, unless the turbulent eddies become quite elongated, this noise source contributes predominantly to the broadband spectrum.

## INTRODUCTION

The noise generated by single-stage subsonic fans consists of a number of discrete tones (predominantly at the blade passing frequency) superimposed on a broadband spec-

trum. It is generally accepted that the broadband noise is generated by such factors as interaction of the blades with patches of inlet turbulence, irregular vortex shedding by the fan blades, and random modulation of rotor wakes impinging on a downstream stator. The discrete tones are believed to be caused by periodic spatial nonuniformities entering the fan and by the passage of its wakes across the stator. However, if the blade passing frequency is large compared with the characteristic turbulence frequency, the sound generated by the inlet turbulence interaction will be concentrated around the harmonics of the blade passing frequency and the spectrum will appear to contain tones of finite width. Thus, the inlet turbulence interaction may also contribute to the pure tones.

This report is concerned with the sound generated by the interaction of inflow turbulence with a high-speed compressor fan. The turbulence in the flow entering a compressor fan (both in the casing boundary layer and in the main stream) can produce noise through two mechanisms. One is a quadrupole-like mechanism which is the result of the fluctuating Reynolds stresses in the volume exterior to the blades produced by the interaction of the turbulence with the potential-flow field of the rotor. The other is a dipole-like interaction which is the result of the fluctuating lift on the fan blade resulting from the fluctuations in angle of attack caused by the turbulence.

Until fairly recently, all analyses of fan noise considered only the dipole mechanism. However, at the operating Mach numbers of modern fans the quadrupole interaction is probably dominant.

Analyses of the inlet turbulence noise generated through the dipole mechanism have been given by Sevik (ref. 1) and Mani (ref. 2). The possibility that this noise is generated through a quadrupole mechanism was first pointed out by Ffowcs-Williams and Hawkings (ref. 3) and was later investigated in detail for a low-speed fan by Chandrashekara (ref. 4). Chandrashekara carried out a combined theoretical and experimental investigation of a low-speed (tip Mach number less than 0.3) unducted fan. He compared the "tone" noise predicted by both his analysis and the dipole analysis of Mani (ref. 2) with his measurements and found that the level of the tones predicted by the quadrupole model was considerably below the experimental values, while the dipole model predicted the correct level. However, the ratio of the quadrupole noise to the dipole noise should vary as Mach number squared and should increase with increased blade loading (ref. 4). Hence, at the high tip speeds and blade loadings at which current jet engine fans operate, it is likely that the quadrupole mechanism will dominate. However, even though inlet turbulence is a dominant noise source in fans, no quadrupole model suitable for high subsonic Mach numbers is available for calculating this noise. The present report is written to fill this gap.

In order to construct a model which applies to a ducted fan at these high speeds, it is necessary to use a model which differs from the one used by Chandrashekara in a number of important respects. First, the present model considers a fan operating in an infinite duct containing a mean axial flow and not in free space with zero mean flow. In

Chandrashekara's analysis the variation in retarded time across the turbulent eddy was neglected. However, as pointed out by Ffowcs-Williams and Hawkings (ref. 3), this is not a good approximation at high tip Mach numbers, especially for the "tone" noise, since the sound is concentrated at the blade passing frequency, which is quite high, and hence corresponds to a condition where the wavelength of the sound can be smaller than the "eddy" size. Thus, this omission also serves to limit Chandrashekara's analysis to low Mach numbers. The present analysis also explicitly accounts for the convection of the eddies by the mean flow, which from studies of jet noise is found to be important for properly modeling the turbulence. In the present analysis the effects of compressibility on the rotor potential-flow field are included. This is important because of the high Mach numbers of interest. A more detailed model of this flow field is also adopted. In real turbulent flows the turbulence is not isotropic, but the eddies tend to be elongated in the direction of flow. Since the flow into a stationary inlet involves a large convergence of the streamlines, it has been argued that the turbulent eddies can become quite elongated in the direction of flow. We have therefore adopted a turbulence model which is general enough to account for this effect.

The analysis leads to a formula for the power spectral density of the sound field emitted through the fan inlet as a function of various aerodynamic and geometric parameters of the fan and the properties of the inlet turbulence. This formula cannot only be used for incorporating the quadrupole inlet turbulence noise into fan noise calculation packages and acoustic liner design programs, but should also be useful for making parametric studies of the sound field produced by this noise source. Hence, numerical results are computed for parameters covering the design range of the various Quiet Fans which have been tested at Lewis. The predicted spectra exhibit a number of features which are observed in the spectra of actual fans. But it is found that the width of the tones predicted by the analysis will generally be broader than those observed in the fan spectrum unless the turbulent eddies are quite elongated (typically of the order of a couple of feet). However, there is mounting evidence that the turbulent eddies drawn into a nontranslating fan do indeed become very elongated and as a result are the dominant source of pure tones in turbojet engines on the ground. This elongation does not occur during forward flight and, in fact, recent measurements by Cumpsty and Lowery (ref. 5) indicate that the tones produced by aircraft engine fans are considerably reduced in flight. The present analysis should be helpful in resolving this question.

## ANALYSIS

### Basic Formulas for Quadrupole Sound Emission

It is shown in reference 6 that the density fluctuation $\rho'(\vec{x}, t)$ at the point $\vec{x}$ and the time $t$ due to the quadrupole radiation from a fan in an infinite duct containing a uniform

axial flow with velocity $U$ is governed by the equation

$$\rho'(\vec{x}, t) = \frac{1}{c_0^2} \int_{-\infty}^{\infty} \int_{\nu(\tau)} \frac{\partial^2 G}{\partial y_i \, \partial y_j} T_{ij}^{\dagger} \, d\vec{y} \, d\tau \tag{1}$$

where $c_0$ is the speed of sound, $\tau$ is the time,

$$T_{ij}^{\dagger}(\vec{y}, \tau) \equiv \rho v_i^{\dagger} v_j^{\dagger} + \delta_{ij}\left(p - c_0^2 \rho'\right) - e_{ij} \tag{2}$$

is Lighthill's stress tensor based on the relative velocity

$$v_i^{\dagger} \equiv v_i - \delta_{1i} U \tag{3}$$

instead of the actual velocity $v_i$, $p$ is the pressure measured above the ambient pressure $p_0$, and $e_{ij}$ is the viscous stress tensor. (All symbols are defined in appendix B.) The volume $\nu(\tau)$ over which the integration is carried out is the entire region of the duct external to the blades. The uniformly moving medium, outgoing-wave, infinite-duct Green's function $G$ is given by (ref. 6)

$$G(\vec{y}, \tau \,|\, \vec{x}, t) = \frac{i}{4\pi} \sum_{m, n} \frac{\Phi_{m, n}(y_2, y_3) \overline{\Phi_{m, n}(x_2, x_3)}}{\Gamma_{m, n}}$$

$$\times \int_{-\infty}^{\infty} \frac{\exp\left\{i\left[\omega(\tau - t) + \left(\frac{Mk}{\beta^2}\right)(y_1 - x_1) + \left(\frac{k_{m, n}}{\beta^2}\right)|y_1 - x_1|\right]\right\}}{k_{m, n}} d\omega \tag{4}$$

where $k = \omega/c_0$, $M = U/c_0$, $\beta = \sqrt{1 - M^2}$, and $\Phi_{m, n}$ denotes a doubly infinite set of eigenfunctions with eigenvalues $\kappa_{m, n}$ determined by solving the Helmholtz equation

$$\left(\frac{\partial^2}{\partial y_2^2} + \frac{\partial^2}{\partial y_3^2}\right)\Phi_{m, n} + \kappa_{m, n}^2 \Phi_{m, n} = 0 \tag{5}$$

on the cross-sectional area $A$ of the duct subject to appropriate homogeneous boundary conditions on the duct surface. Thus, when the surface of the duct is rigid, we must require that

$$\frac{\partial \Phi_{m,n}}{\partial n} = 0 \qquad \text{on } S \tag{6}$$

where $\partial/\partial n$ denotes the normal derivative to the duct surface $S$. The remaining quantities in equation (4) are

$$\Gamma_{m,n} \equiv \int_A |\Phi_{m,n}|^2 \, dy_2 \, dy_3 \tag{7}$$

and

$$k_{m,n} \equiv \sqrt{k^2 - \beta^2 \kappa_{m,n}^2}$$

where, in order to ensure that $G$ represents the outgoing-wave Green's function, we must choose the branch out of the square root to be as shown in figure 1.

When the observation point $\vec{x}$ is far enough from the source (i.e., in the far field), the pressure and density fluctuations will be small and we can use the linear approximation

$$p = c_0^2 \rho' \tag{8}$$

## Rectangular Duct Model

In order to model a real fan, the most appropriate cross-sectional shape of the duct is an annulus such as that shown in figure 2(a). The eigenfunctions $\Phi_{m,n}$ will then be combinations of Bessel functions. The analysis can be considerably simplified, however, by assuming that the duct is "unrolled" into the rectangular strip shown in figure 2(b). (The larger the number of blades, the more closely the rotor approximates a two-dimensional disturbance pattern with subsonic phase speed.) The width $\delta$ of the rectangular duct is equal to $2\pi$ times the mean radius $\bar{R}$ of the annular duct, and its height $b$ is equal to the outer radius minus the inner radius of the annular duct. In this case we must require that $\Phi_{m,n}$ and its normal derivative take on the same values on the surface $S_a$ as they do on the corresponding points on the surface $S_b$ (periodicity conditions). It is easy to verify that the eigenfunctions of equation (5) which satisfy this

condition together with the boundary condition (6) on the upper and lower walls are given by

$$\Phi_{m,n} = e^{i2\pi m y_2/\delta} \cos \frac{n\pi y_3}{b} \qquad \text{for} \begin{cases} n = 0, 1, 2, \ldots \\ m = 0, \pm 1, \pm 2, \ldots \end{cases}$$

where the y-coordinate system is shown in figure 3 and the corresponding eigenvalues are given by

$$\kappa_{m,n}^2 = \left[\left(\frac{2m}{\delta}\right)^2 + \left(\frac{n}{b}\right)^2\right]\pi^2 \tag{9}$$

Hence,

$$k_{m,n} = \sqrt{k^2 - \beta^2\pi^2\left[\left(\frac{2m}{\delta}\right)^2 + \left(\frac{n}{b}\right)^2\right]} \tag{10}$$

$$\Gamma_{m,n} = \int_0^{\delta}\int_0^{b} \cos^2 \frac{n\pi y_3}{b}\, dy_2\, dy_3 = \frac{\delta b}{2}(1 + \delta_{n,0})$$

and

$$G(\vec{y}, \tau \,|\, \vec{x}, t) = \frac{i}{2\pi\delta b} \sum_{m=-\infty}^{\infty} \sum_{n=0}^{\infty} \frac{\cos \frac{n\pi y_3}{b} \cos \frac{n\pi x_3}{b}}{1 + \delta_{n,0}} e^{i2m\pi(y_2 - x_2)/\delta}$$

$$\times \int_{-\infty}^{\infty} \frac{\exp\left\{-i\left[\omega(t - \tau) - \left(\frac{1}{\beta^2}\right)(Mk \pm k_{m,n})(y_1 - x_1)\right]\right\}}{k_{m,n}} d\omega \tag{11}$$

where the upper sign corresponds to upstream propagation ($x_1 < y_1$) and the lower sign corresponds to downstream propagation ($x_1 > y_1$).

## Transformation to Rotor Coordinates

In order to make the limits of integration in equation (1) independent of time, we introduce the $\vec{\eta}$-coordinate system by

$$\eta_i = y_i + \delta_{i2} U_t \tau \tag{12}$$

where $U_t$ denotes the velocity of the blade row and is taken as positive in the direction shown in figure 3. But since for each value of $(y_1, y_3)$ $T_{ij}^{\dagger}$ takes on the same value at $y_2 = -\delta/2$ as it does at $y_2 = +\delta/2$, it can be extended to a continuous periodic function from $-\infty$ to $+\infty$. And since the Green's function is also periodic, the integration with respect to $\eta_2$ can be carried out over any region $\nu_0$ of fixed shape which coincides with $\nu(\tau)$ at some definite instant of time. Hence, equation (1) becomes

$$p(\vec{x}, t) = \int_{-\infty}^{\infty} \int_{\nu_0} \frac{\partial^2 G}{\partial \eta_i \, \partial \eta_j} T_{ij}^{\dagger}(\vec{\eta}, \tau) d\vec{\eta} \, d\tau \tag{13}$$

where the linear approximation (8) has been used.

## Derivation of Spectral Equations

Rather than deal with the pressure directly, it is convenient to deal with its spectrum $P(\omega)$ defined by the generalized Fourier transform

$$p = \int_{-\infty}^{\infty} P(\omega) e^{-i\omega t} \, d\omega \tag{14}$$

It then follows upon inserting equation (12) into equation (11) and using the result in equation (13) that

$$P(\omega) = \sum_{m=-\infty}^{\infty} \sum_{n=0}^{\infty} P^{\pm}_{m,n}(\omega) C^{\pm}_{m,n}(\vec{x}) \tag{15}$$

where

$$P^{\pm}_{m,n} = \int_{\nu_0} \left[ \frac{\partial^2}{\partial \eta_i \, \partial \eta_j} e^{i\left(\alpha_1^{\pm}\eta_1 + \alpha_2^{\pm}\eta_2\right)} \cos\left(\alpha_3^{\pm}\eta_3\right) \right] \int_{-\infty}^{\infty} e^{i(\omega - 2m\pi U_t/\delta)\tau} \, T^{\dagger}_{ij} \, d\tau \, d\vec{\eta} \tag{16}$$

$$\left.\begin{aligned} \alpha_1^{\pm} &\equiv \frac{1}{\beta^2}\left(Mk \pm k_{m,n}\right) \\ \alpha_2^{\pm} &= 2m\pi/\delta \\ \alpha_3^{\pm} &= n\pi/b \end{aligned}\right\} \tag{17}$$

$$C^{\pm}_{m,n} = \frac{i}{2\pi\delta b} \frac{\cos\left(\frac{n\pi x_3}{b}\right)}{(1 + \delta_{n,0})k_{m,n}} \exp\left\{-i\left[\left(\frac{1}{\beta^2}\right)\left(Mk \pm k_{m,n}\right)x_1 + \frac{2m\pi x_2}{\delta}\right]\right\} \tag{18}$$

and the plus sign corresponds to upstream propagation while the minus sign corresponds to downstream propagation.

## Radiated Acoustic Power

The quantity which is perhaps of most interest is the total acoustic power per unit frequency $\mathscr{P}^{\pm}$ radiated (upstream/downstream). This can be calculated by integrating the axial component $\bar{I}_{\omega}(\vec{x})$ of the intensity spectrum over the cross-sectional area of the duct. Thus, [1]

[1]The factor 2 arises because both $\bar{I}_{\omega}$ and $\bar{I}_{-\omega}$ contribute to the acoustic power with frequency $\omega$. Since $\bar{I}_{\omega}$ arises as a Fourier transform, it is defined for positive and negative frequencies. But since $\bar{I}_{\omega} = \bar{I}_{-\omega}$ and the experimental power is defined only for positive frequencies, the factor of 2 must be included.

$$\mathcal{P}^{\pm}(\omega) = \lim_{x_1 \to \infty} 2 \int_{-\delta/2}^{\delta/2} \int_0^b \bar{I}_\omega(\vec{x}) dx_2\, dx_3 \tag{19}$$

We shall suppose that the sound field is time stationary. Then it is shown in reference 6 that

$$\bar{I}_\omega = \lim_{T \to \infty} \frac{2\pi}{T} \left[ (1 + M^2) P \bar{V} + \frac{M}{\rho_0 c_0} |P|^2 + \rho_0 c_0 M |V|^2 \right] \tag{20}$$

where T is the integration time for the Fourier transform and V is the generalized Fourier transform of the axial acoustic velocity $v_1^{\dagger}(x, t)$. Thus, since p and $v_1^{\dagger}$ obey the linearized acoustic equations at large distances from the fan

$$-\frac{\partial p}{\partial x_1} = \rho_0 \left( \frac{\partial}{\partial t} + c_0 M \frac{\partial}{\partial x_1} \right) v_1$$

Hence,

$$-\frac{\partial P}{\partial x_1} = -\rho_0 c_0 \left( ik - M \frac{\partial}{\partial x_1} \right) V$$

Inserting equations (15) and (17) into this relation shows that

$$V = \frac{1}{\rho_0 c_0} \sum_{m=-\infty}^{\infty} \sum_{n=0}^{\infty} \lambda_{m,n}^{\pm} P_{m,n}^{\pm}(\omega) C_{m,n}^{\pm}(\vec{x}) \tag{21}$$

where

$$\lambda_{m,n}^{\pm} = -\frac{Mk \pm k_{m,n}}{k \pm M k_{m,n}} \tag{22}$$

Since equation (18) shows that

$$\int_{-\delta/2}^{\delta/2} \int_0^b C_{m,n} \bar{C}_{p,q}\, dx_2\, dx_3 = \frac{\delta_{m,p} \delta_{n,q}}{8\pi^2 \delta b k_{m,n}^2 (1 + \delta_{n,0})}$$

Substituting equations (15) and (21) into equation (20) and using the result in equation (19) show that

$$\mathscr{P}^{\pm}(\omega) = \frac{\mp\beta^4 k}{4\pi^2\rho_0 c_0 \delta b} \sum_{\substack{\text{(All } m \text{ and} \\ \text{all } n\geq 0 \text{ with} \\ k^2>\beta^2\kappa_{m,n}^2)}} \frac{\Omega_{m,n}^{\pm}}{(1+\delta_{n,0})k_{m,n}\left(k \pm Mk_{m,n}\right)^2} \tag{23}$$

where, since cutoff modes do not contribute to equation (23), the sum in this equation is carried out only over propagating modes and

$$\Omega_{m,n}^{\pm} \equiv \lim_{T\to\infty} \frac{2\pi}{T} \left|P_{m,n}^{\pm}(\omega)\right|$$

Inserting equation (16) into this relation shows upon using the Wiener-Khinchin relations for stationary processes

$$\Omega_{m,n} = 2\pi \int_{\nu_0}\int_{\nu_0} \left( \frac{\partial^4 \exp\left\{i\left[\alpha_1^{\pm}(\eta_1 - \eta_1') + \alpha_2^{\pm}(\eta_2 - \eta_2')\right]\right\} \cos(\alpha_3^{\pm}\eta_3)\cos(\alpha_3^{\pm}\eta_3')}{\partial\eta_i\,\partial\eta_j\,\partial\eta_k'\,\partial\eta_l'} \right)$$

$$\times \int_{-\infty}^{\infty} e^{-i(\omega - 2m\pi U_t/\delta)\tau} \mathscr{R}_{ijkl}\, d\tau\, d\vec{\eta}\, d\vec{\eta}' \tag{24}$$

where

$$\mathscr{R}_{ijkl}(\vec{\eta}, \vec{\eta}', \tau) \equiv \overline{T_{ij}^{\dagger}(\vec{\eta}, t) T_{kl}^{\dagger}(\vec{\eta}', t+\tau)} \tag{25}$$

and the overbar denotes the time average

$$\bar{f} \equiv \lim_{T\to\infty} \frac{1}{T} \int_{-T/2}^{T/2} f(t)dt \tag{26}$$

## Source Model

In order to use these results to predict the sound emission, it is necessary to determine the source term $\mathscr{R}_{ijkl}$. As in any aeroacoustic problem, this is extremely difficult to do exactly since it requires a knowledge of the complete flow including the acoustic field. It is therefore customary in aeroacoustic problems to develop an approximate model for the source term. In this section the general structure of this source model will be evolved, and it will be used at the end of the section to simplify the equations derived in the preceding section. The source model will involve contributions from the turbulence and the phase-locked rotor velocity field. In the next section a model for the rotor velocity field will be developed, and the results will be used in subsequent sections to simplify the formulas for the sound field. A model for the turbulence correlation tensor will then be introduced, and with this in hand the final equations will be derived in the last section.

As a first step in evolving the source model, we shall replace Lighthill's stress tensor $T_{ij}^{\dagger}$ by the Reynolds stress (ref. 7). (This procedure is followed in most analyses which do not involve combustion.)

$$T_{ij}^{\dagger} = \rho_0 v_i^{\dagger} v_j^{\dagger} \tag{27}$$

We shall further assume that the relative velocity $v_i^{\dagger}$ can be decomposed into the sum of a random fluctuating velocity $u_i$ (with zero mean) associated with the inlet turbulence and a velocity $w_i$ associated with the phase-locked rotor pressure field. Then $w_i$ is independent of time in the $\vec{\eta}$-coordinate system and

$$v_i^{\dagger}(\vec{\eta}, t) = u_i(\vec{\eta}, t) + w_i(\vec{\eta}) \tag{28}$$

$$\overline{u_i} = 0 \tag{29}$$

where $u_i$ and $w_i$ denote velocities relative to a coordinate system moving uniformly in the $y_1$-direction even though they are expressed as functions of the rotor-locked $\vec{\eta}$-coordinate system.

Inserting equation (28) into equation (27) and using the result in equation (25) shows that

$$\frac{\mathscr{R}_{ijk\ell}}{\rho_0^2} = R_{ijk\ell} + R_{ik}w_j w'_\ell + R_{jk}w_i w'_\ell + R_{i\ell}w_j w'_k + R_{j\ell}w_i w'_k$$

$$+ R_{ij,k}w'_\ell + R_{ij,\ell}w'_k + R_{i,k\ell}w_j + R_{j,\ell k}w_i + \text{Time-independent terms} \qquad (30)$$

where

$$R_{ijk\ell} = \overline{u_i u_j u'_k u'_\ell}$$

$$R_{ij,k} = \overline{u_i u_j u'_k}$$

$$R_{i,jk} = \overline{u_i u'_j u'_k}$$

$$R_{ij} = \overline{u_i u'_j}$$

are turbulence velocity correlations and the unprimed quantities are evaluated at $\vec{\eta}$ and $t$ while the primed quantities are evaluated at $\vec{\eta}'$ and $t + \tau$.

When the integral with respect to $\tau$ in equation (24) is carried out over the time-independent terms, it will yield a term proportional to $\delta(\omega - 2m\pi U_t/\delta)$. But as long as relative Mach number $\sqrt{M^2 + (U_t/c_0)^2}$ is less than unity, $k^2$ will be less than $\beta^2\kappa_{m,n}$ with $\omega = 2m\pi U_t/\delta$ and all modes will be cut off. Hence, for subsonic rotors the time-independent terms will make no contribution to the sound field and can be omitted.

We shall assume (as is usual in compressor analyses) that the phase-locked rotor flow field is two dimensional so that $w_j$ is independent of $y_3 = \eta_3$. It is convenient to introduce the new variables

$$\vec{\xi} \equiv \vec{\eta}' - \vec{\eta} \qquad (31)$$

$$Y \equiv \left(\eta_1,\ \eta_2,\ \frac{\eta'_3 + \eta_3}{2}\right)$$

We shall now suppose that the turbulence is homogeneous. Then $\mathscr{R}_{ijk\ell}$ (considered as a function of $\vec{\xi}$ and $\vec{Y}$) will be independent of $Y_3$. We shall also suppose that the region of integration can be extended to the interior of the blade row and that the turbu-

lence correlation length in the $y_2$- and $y_3$-directions is small compared with the lengths of $\delta$ and $b$ in those directions. Then the integration with respect to $\vec{\xi}$ can be carried out over all space and the integration with respect to $\vec{Y}$ carried out over $\nu_0$. (Hence, upon using the identity)

$$\cos\left(\frac{n\pi}{b}\eta_3\right)\cos\left(\frac{n\pi}{b}\eta_3'\right) = \frac{1}{2}\left(\cos\frac{n\pi\xi_3}{b} + \cos\frac{2n\pi Y_3}{b}\right)$$

equation (24) becomes

$$\Omega^{\pm}_{m,n} = \pi \iint_{\infty}\iint_{\nu_0} \frac{\partial^4 e^{-i\left(\alpha_1^{\pm}\xi_1+\alpha_2^{\pm}\xi_2\right)}\left(\cos\frac{n\pi\xi_3}{b} + \cos\frac{2n\pi Y_3}{b}\right)}{\partial\eta_i\,\partial\eta_j\,\partial\eta_k'\,\partial\eta_l'}$$

$$\times \int_{-\infty}^{\infty} e^{-i(\omega-2m\pi U_t/\delta)\tau}\,\mathscr{R}_{ijkl}\,d\tau\,d\vec{\xi}\,d\vec{Y} \qquad (32)$$

where the notation $\int_{\infty}$ indicates that the integration is to be carried out over all space. Now the only term depending on $Y_3$ is $\cos(2n\pi Y_3/b)$, and the integration with respect to this variable is from 0 to $b$. But since $\cos(2n\pi Y_3/b)$ and all its derivatives integrate to zero over this range whenever $n \neq 0$, we can carry out the integration with respect to $Y_3$ in equation (32) to obtain

$$\Omega^{\pm}_{m,n} = \pi(1+\delta_{n,0})b \iint_{\infty}\iint_{A_0} \frac{\partial^4 e^{-i\left(\alpha_1^{\pm}\xi_1+\alpha_2^{\pm}\xi_2\right)}\cos\alpha_3^{\pm}\xi_3}{\partial\xi_i\,\partial\xi_j\,\partial\xi_k\,\partial\xi_l}$$

$$\times \int_{-\infty}^{\infty} e^{-i(\omega-2m\pi U_t/\delta)\tau}\,\mathscr{R}_{ijkl}\,d\tau\,d\vec{\xi}\,d\eta_2\,d\eta_1 \qquad (33)$$

where $A_0$ denotes the cross-sectional area of any plane, $y_3$ = Constant, included between the duct walls and the exterior of the blades.

The first term on the right side of equation (30) represents the effect of the interaction of the turbulence with itself. This noise generation mechanism is the same as that which produces jet noise and is known to be a highly inefficient producer of sound relative to the other noise mechanisms which are present (refs. 3 and 7). We shall therefore neglect this term. When equation (30) is substituted into equation (33), we therefore obtain after interchanging dummy indices

$$\Omega^{\pm}_{m,n} = 4\pi\rho_0^2 b(1+\delta_{n,0}) \int_{\infty} \frac{\partial^4 e^{-i\,\alpha_1^{\pm}\xi_1+\alpha_2\xi_2^{\pm}} \cos\alpha_3^{\pm}\xi_3}{\partial\xi_i\,\partial\xi_j\,\partial\xi_k\,\partial\xi_l}$$

$$\times \left[ H_{jl} \int_{-\infty}^{\infty} R_{ik}\, e^{-i(\omega-2m\pi U_t/\delta)\tau}\, d\tau + \frac{1}{2} H_j \int_{-\infty}^{\infty} R_{i,kl}\, e^{-i(\omega-2m\pi U_t/\delta)\tau}\, d\tau \right.$$

$$\left. + \frac{1}{2} H'_l \int_{-\infty}^{\infty} R_{ij,k}\, e^{-i(\omega-2m\pi U_t/\delta)\tau}\, d\tau \right] d\vec{\xi} \tag{34}$$

where the rotor velocity integrals $H_{jl}$, $H_j$, and $H'_j$ are defined by

$$H_{jl} \equiv \int_{A_0} w_j w'_l\, d\eta_2\, d\eta_1 \tag{35}$$

$$\left.\begin{aligned} H_j &\equiv \int_{A_0} w_j\, d\eta_2\, d\eta_1 \\ H'_j &\equiv \int_{A_0} w'_j\, d\eta_2\, d\eta_1 \end{aligned}\right\} \tag{36}$$

## Rotor Velocity Field Model

We shall now develop an approximate model for the phase-locked rotor velocity field $w_j$. Most fan blades have fairly small camber, and linearized theory can be used. But

since the quadrupole source is of interest at high subsonic Mach numbers, we must take into account the effects of compressibility. It is convenient to introduce the $\vec{X}$-coordinate system, which is alined with the blades as shown in figure 4. It is well known that the potential-flow field about such a blade row can be represented by a uniform velocity plus a distribution of line vortices along the blade chords. In order to simplify the analysis, we replace this vortex distribution by a discrete set of concentrated vortices lying at the midchord point. Let $V_1$ and $V_2$ denote the velocity components along the $X_1$- and $X_2$-directions, respectively (relative to the blades). Then according to linearized theory the velocity induced by a single compressible vortex of strength $\Gamma_0$ at the origin is given by

$$V_1 - i\frac{V_2}{\beta_r} = \frac{\Gamma_0}{2\pi_i}\frac{1}{Z}$$

where

$$\beta_r \equiv \sqrt{1 - \left(\frac{U_r}{c_0}\right)^2} \tag{37}$$

and

$$Z = X_1 + i\beta_r X_2 \tag{38}$$

Hence, the concentrated vorticity approximation to the velocity field about the cascade is given by

$$V_1 - i\frac{V_2}{\beta_r} = U_r - i\frac{v_0}{\beta_r} + \frac{\Gamma_0}{2\pi i}\sum_{n=-\infty}^{\infty}\frac{1}{Z - i\Delta_0 n} \tag{39}$$

where $v_0$ is the uniform (in general, complex) velocity (which will be chosen to make the flow far upstream of the cascade equal to $U_r$) and

$$\Delta_0 = \Delta(\beta_r \cos\gamma - i \sin\gamma) \tag{40}$$

where $\Delta$ is the interblade spacing and $\gamma$ is called the stagger angle. But upon using the relation (ref. 8)

$$\sum_{n=-\infty}^{\infty} \frac{1}{Z - in\pi} = \coth Z$$

equation (39) becomes

$$V_1 - i\frac{V_2}{\beta_r} = U_r - i\frac{v_0}{\beta_r} + \frac{\Gamma_0}{2\Delta_0 i}\coth\frac{\pi Z}{\Delta_0}$$

But since

$$\lim_{X_1 \to -\infty} \coth\frac{\pi Z}{\Delta_0} = -1$$

we must put

$$\frac{v_0}{\beta_r} = \frac{\Gamma_0}{2\Delta_0}$$

Hence,

$$V_1 - i\frac{V_2}{\beta_r} = U_r + \frac{\Gamma_0}{i2\Delta_0}\left(1 + \coth\frac{\pi Z}{\Delta_0}\right) \tag{41}$$

It can be seen from figure 4 that the $X_1, X_2$ coordinate system is related to the rotating $\eta_1, \eta_2$ duct alined coordinates by

$$X_1 = \eta_1 \cos\gamma + \eta_2 \sin\gamma$$

$$X_2 = -\eta_1 \sin\gamma + \eta_2 \cos\gamma$$

Hence, it follows from equations (38) and (40) that

$$\frac{Z}{\Delta_0} = \frac{\eta_1(\cos\gamma - i\beta_r \sin\gamma)}{\Delta(\beta_r \cos\gamma - i \sin\gamma)} + i\frac{\eta_2}{\Delta}$$

$$= \frac{\eta_1\left[\beta_r + i\left(1 - \beta_r^2\right)\sin\gamma \cos\gamma\right]}{\Delta\left(\beta_r^2 \cos^2\gamma + \sin^2\gamma\right)} + i\frac{\eta_2}{\Delta}$$

But upon using the velocity triangle in figure 4, this can be written as

$$\frac{Z}{\Delta_0} = \frac{z}{\Delta} \tag{42}$$

where

$$z = \eta_1 D + i\eta_2 \tag{43}$$

$$D \equiv \frac{\beta_r + iMM_t}{\beta^2} \tag{44}$$

and

$$M_t \equiv \frac{U_t}{c_0} \tag{45}$$

is the Mach number of the blade row.

The velocity components $w_1$ and $w_2$ are in the $\eta_1$- and $\eta_2$-directions and are measured relative to a reference frame moving with a uniform velocity U in the $\eta_1$-direction, while the velocities $V_1$ and $V_2$ are in the $X_1$- and $X_2$-directions and are measured in a reference frame moving with the cascade velocity $U_t$. Hence, it follows from figure 4 that

$$V_1 = (w_1 + U)\cos\gamma + (w_2 + U_t)\sin\gamma$$

$$V_2 = (w_2 + U_t)\cos\gamma - (w_1 + U)\sin\gamma$$

$$= w_2 \cos\gamma - w_1 \sin\gamma$$

Then

$$(\beta_r \cos\gamma - i \sin\gamma)\left(V_1 - i\frac{V_2}{\beta_r} - U_r\right) = \frac{w_1\beta^2 - iw_2\bar{D}}{\beta_r}$$

Multiplying equation (41) through by $(\beta_r \cos\gamma - i \sin\gamma)\beta_r$ and using equations (40) and (42) show that

$$\beta^2(w_1 - iw_2\bar{D}) = \frac{\Gamma_0\beta_r}{2i\Delta}\left(1 + \coth\frac{\pi z}{\Delta}\right) \tag{46}$$

Then

$$\lim_{\eta_1 \to +\infty} \beta^2(w_1 - iw_2\bar{D}) = \frac{\Gamma_0}{2i\Delta}$$

Equating the imaginary parts of this expression shows that $\Delta w_2$, the change in $w_2$ across the blade row, is related to $\Gamma_0$ by

$$\frac{\Gamma_0}{\Delta} = \Delta w_2 = -U_t\theta$$

where $\theta \equiv -\Delta w_2/U_t$ is called the work coefficient of the ran. Hence, equation (46) can be written as

$$\beta^2(w_1 - iw_2\bar{D}) = \frac{i\theta\beta_r U_t}{2}\left(1 + \coth\frac{\pi z}{\Delta}\right)$$

$$= \frac{i\theta\beta_r U_t}{2}\,\frac{e^{\pi z/\Delta}}{\sinh\frac{\pi z}{\Delta}}$$

By using the geometric series

$$\frac{1}{1 - z} = \sum_{p=0}^{\infty} z^p \qquad \text{for } |z| < 1$$

(with $z \to \exp(\pm 2\pi z/\Delta)$), this becomes

$$\beta^2(w_1 - iw_2\bar{D}) = \begin{cases} -iU_t\beta_r\theta \sum_{p=1}^{\infty} e^{2\pi pz/\Delta} & \text{if } \eta_1 < 0 \\ iU_t\beta_r\theta \sum_{p=0}^{\infty} e^{-2\pi pz/\Delta} & \text{if } \eta_1 > 0 \end{cases}$$

Equating real and imaginary parts now shows that

$$w_1\beta^2 - w_2 M_t M = \frac{-iU_t\theta\beta_r}{2} \sum_{p=1}^{\infty} (e^{2\pi pz/\Delta} - e^{2\pi p\bar{z}/\Delta}) \qquad \text{for } \eta_1 < 0$$

$$w_2 = \frac{U_t\theta}{2} \sum_{p=1}^{\infty} (e^{2\pi pz/\Delta} + e^{2\pi p\bar{z}/\Delta}) \qquad \text{for } \eta_1 < 0 \tag{47}$$

Or adding the results

$$w_1 = \frac{-iU_t\theta}{2} \sum_{p=1}^{\infty} (De^{2\pi pz/\Delta} - \bar{D}e^{2\pi p\bar{z}/\Delta}) \qquad \text{for } \eta_1 < 0 \tag{48}$$

The noise generated by inlet turbulence probably has its largest effect on the sound field passing through the fan inlet. We shall therefore restrict our attention to the upstream-propagating waves. We shall also suppose that only the front half of the cascade potential-flow field is effective in interacting with the inlet turbulence and generating sound which propagates upstream. Hence we set

$$w_1 = w_2 = 0 \qquad \text{for } \eta_1 > 0 \tag{49}$$

## Evaluation of Rotor Velocity Field Integrals

The results of the previous section will now be used to evaluate the integrals defined by equations (35) and (36). It follows from equations (47) and (48) and the orthogonality properties of the complex exponentials that

$$H_j = H_j' = 0 \tag{50}$$

Next (in order to facilitate the analysis) we define the rotor velocity correlations by

$$L_{jl} \equiv \int_{-\delta/2}^{\delta/2} w_j(\vec{\eta}) w_l(\vec{\eta} + \vec{\xi}) d\eta_2 \tag{51}$$

Equation (35) shows that

$$H_{jl} = \int_{-\infty}^{\infty} L_{jl}\, d\eta_1 \tag{52}$$

provided we extend the region of integration to the interior of the blades. Inserting equations (47) and (48) into equation (51) now shows that for

$$\eta_1 < \min\{-\xi_1, 0\}$$

$$L_{21} = \frac{\delta U_t^2 \theta^2}{2} \mathcal{I}m \sum_{p=1}^{\infty} D \exp \frac{2\pi p}{\Delta}\left[\left(\frac{2\beta_r}{\beta^2}\right)\eta_1 + D\xi_1 + i\xi_2\right]$$

$$L_{12} = -\frac{\delta U_t^2 \theta^2}{2} \mathcal{I}m\, \bar{D} \sum_{p=1}^{\infty} \exp \frac{2\pi p}{\Delta}\left[\left(\frac{2\beta_r}{\beta^2}\right)\eta_1 + D\xi_1 + i\xi_2\right]$$

$$L_{22} = \frac{\delta U_t^2 \theta^2}{2} \mathcal{R}e \sum_{p=1}^{\infty} \exp \frac{2\pi p}{\Delta}\left[\left(\frac{2\beta_r}{\beta^2}\right)\eta_1 + D\xi_1 + i\xi_2\right]$$

$$L_{11} = |D|^2 L_{22} = \frac{1 - M_t^2}{\beta^2} L_{22}$$

and

$$L_{jl} = 0$$

otherwise. Inserting these results into equation (52) now shows that

$$H_{11} = \frac{1 - M_t^2}{\beta^2} H_{22}$$

$$= \frac{\delta U_t^2 \theta^2}{2} \left( \frac{1 - M_t^2}{\beta_r} \right) \sum_{p=1}^{\infty} \frac{\Delta}{4\pi p} \exp\left[ - \left( \frac{\beta_r}{\beta^2} \right) |\xi_1| \frac{2\pi p}{\Delta} \right] \mathcal{R}e \exp\left\{ i \left( \frac{2\pi p}{\Delta} \right) \left[ \left( \frac{MM_t}{\beta^2} \right) \xi_1 + \xi_2 \right] \right\} \tag{53}$$

$$H_{21} = \frac{\delta U_t^2 \theta^2 \beta^2}{2\beta_r} \sum_{p=1}^{\infty} \frac{\Delta}{4\pi p} \exp\left[ - \left( \frac{\beta_r}{\beta^2} \right) |\xi_1| \frac{2\pi p}{\Delta} \right] \mathcal{I}m D \exp\left\{ i \left( \frac{2\pi p}{\Delta} \right) \left[ \left( \frac{MM_t}{\beta^2} \right) \xi_1 + \xi_2 \right] \right\} \tag{54}$$

$$H_{12} = - \frac{\delta U_t^2 \theta^2 \beta^2}{2\beta_r} \sum_{p=1}^{\infty} \frac{\Delta}{4\pi p} \exp\left[ - \left( \frac{\beta_r}{\beta^2} \right) |\xi_1| \frac{2\pi p}{\Delta} \right] \mathcal{I}m \bar{D} \exp\left\{ i \left( \frac{2\pi p}{\Delta} \right) \left[ \left( \frac{MM_t}{\beta^2} \right) \xi_1 + \xi_2 \right] \right\} \tag{55}$$

## Development of Equation for Upstream Sound Propagation

Inserting equation (50) and equations (53) to (55) into equation (34) (with the plus sign only) now shows that

$$\Omega_{m,n}^{+} = \sum_{p=1}^{\infty} \Omega_{m,n}^{p} \tag{56}$$

where

$$\Omega_{m,n}^{p} = \frac{2\pi \rho_0^2 \delta b U_t^2 \theta^2}{\beta_r} (1 + \delta_{n,0}) \alpha_0^2 \alpha_i \alpha_k \int_{\infty} e^{-i(\alpha_1 \xi_1 + \alpha_2 \xi_2)} \frac{1}{2} \left[ e^{-i\alpha_3 \xi_3} + e^{i(\alpha_3 \xi_3 + \delta_{3i}\pi + \delta_{3k}\pi)} \right]$$

$$\times \int_{-\infty}^{\infty} R_{ik} e^{-i(\omega - 2m\pi U_t/\delta)\tau} \frac{\Delta}{4\pi p} e^{-(\beta_r/\beta^2)|\xi_2|(2\pi p/\Delta)} \cos\left[ \frac{2\pi p}{\Delta} \left( \frac{MM_t}{\beta^2} \xi_1 + \xi_2 \right) \right] d\vec{\xi}\, d\tau \tag{57}$$

and

$$\alpha_0^2 = \alpha_1^2 + \alpha_2^2 - (M\alpha_2 - M_t\alpha_1)^2 \tag{58}$$

In order to develop a model for the turbulence correlation tensor $R_{ik}$, it is convenient to introduce a coordinate system which "moves with the turbulent eddies." Thus, we introduce the $\zeta$-coordinate system by

$$\zeta_1 = \xi_1 - U_c\tau$$

$$\zeta_2 = \xi_2 - U_t\tau$$

$$\zeta_3 = \xi_3$$

where $U_c$ denotes the convection velocity of the turbulent eddies. It is not necessarily equal to the axial velocity U. Equation (7) can now be written as

$$\Omega^p_{m,n} = \frac{2\pi\rho_0^2 U_t^2\theta^2\delta b(1+\delta_{n,0})\alpha_0^2\alpha_i\alpha_k}{\beta_r}\int e^{-i(\alpha_1\zeta_1+\alpha_2\zeta_2)}\frac{1}{2}\left[e^{-i\alpha_3\zeta_3} + e^{i(\alpha_3\zeta_3+\delta_{3i}\pi+\delta_{3k}\pi)}\right]$$

$$\times\int_{-\infty}^{\infty}\mathscr{R}_{ik}(\vec{\zeta},\tau)\frac{\Delta}{4\pi p}\exp\left[-i(\omega+\alpha_1 U_c)\tau - \left(\frac{\beta_r}{\beta^2}\right)\left|\zeta_1 + U_c\tau\right|\frac{2\pi p}{\Delta}\right]\cos\left\{\frac{2\pi p}{\Delta}\left[\frac{MM_t}{\beta^2}(U_c\tau+\zeta_1)+\zeta_2+U_t\tau\right]\right\}d\vec{\zeta}\,d\tau \tag{59}$$

where

$$\mathscr{R}_{ik}(\vec{\zeta},\tau) \equiv R_{ik}(\vec{\xi},\tau) \tag{60}$$

is the moving-axis turbulence correlation tensor.

## Model for Turbulence Correlation Tensor

In order to proceed, it is necessary to determine the turbulence correlation tensor. We first assume that the moving-axis turbulence correlation tensor factors into space- and time-dependent parts. Thus, we put

$$\mathscr{R}_{ik} = \mathscr{R}^0_{ik}(\vec{\zeta})e^{-|\tau|\omega_f} \tag{61}$$

where $\omega_f^{-1}$ is the decay time of the moving-frame turbulence correlation. Perhaps the simplest assumption which can be made is that the turbulence is isotropic. The most general form of $\mathscr{R}^0_{ik}$ which satisfies the requirements of continuity (i. e., which is kinematically possible) is

$$\mathscr{R}^0_{ik} = \left(f + \frac{1}{2}\zeta\frac{df}{d\zeta}\right)\delta_{ik} - \frac{1}{2\zeta}\frac{\partial f}{\partial \zeta}\zeta_i\zeta_k$$

where f can be any function of the magnitude $\zeta$ of $\vec{\zeta}$ only. A reasonable assumption in the moving frame is that

$$f = \overline{u^2}\, e^{-\zeta^2/l^2} \tag{62}$$

where $l$ is the turbulence correlation length. The turbulence in the inlet of a real fan is probably not at all isotropic, with the eddies probably being elongated in the direction of flow. In order to develop a kinematically possible turbulence model with scale anisotropy, we follow Kraichnan (ref. 9) and note that the correlation tensor $\mathscr{R}^0_{ik}$ is a contravariant tensor of second rank that satisfies the continuity condition

$$\frac{\partial \mathscr{R}^0_{ik}}{\partial \zeta_k} = 0 \tag{63}$$

which is a tensor equation. Then corresponding to the transformation of coordinates

$$\left.\begin{aligned} \tilde{\zeta}_1 &= r^{-1}\zeta_1 \\ \tilde{\zeta}_2 &= \zeta_2 \\ \tilde{\zeta}_3 &= \zeta_3 \end{aligned}\right\} \tag{64}$$

the transformation

$$\left.\begin{aligned} \tilde{\mathscr{R}}^0_{11} &= r^{-2}\mathscr{R}^0_{11} \\ \tilde{\mathscr{R}}^0_{1k} &= r^{-1}\mathscr{R}^0_{1k} \qquad \text{for } k \neq 1 \\ \tilde{\mathscr{R}}^0_{ik} &= \mathscr{R}^0_{ik} \qquad \text{for } i, k \neq 3 \end{aligned}\right\} \tag{65}$$

ensures that if $\tilde{\mathscr{R}}^0_{ik}$ obeys the equation $\partial\tilde{\mathscr{R}}^0_{ik}/\partial\tilde{\xi}_k = 0$, then $\mathscr{R}^0_{ik}$ will obey equation (63) and hence be kinematically realizable. Thus, if we put

$$\tilde{\mathscr{R}}^0_{ik} = \frac{\overline{u_1^2}}{r^2}\left[\left(1 - \frac{\tilde{\xi}^2}{l^2}\right)\delta_{ik} + \frac{\tilde{\xi}_i\tilde{\xi}_k}{l^2}\right]e^{-\tilde{\xi}^2/l^2} \tag{66}$$

the correlation tensor $\mathscr{R}^0_{ik}(\xi)$ will be kinematically realizable (i. e., satisfies continuity) and will represent a turbulent flow where correlation length in the axial ($y_1$) direction is $rl$ while the correlation length in the transverse direction is $l$.

## Rearrangement of Equation for Upstream Sound Propagation

Substituting equations (61), (65), and (66) into equation (59) yields

$$\Omega^p_{m,n} = \frac{2\pi\rho_0^2\delta b U_t^2 \overline{u_1^2}\theta^2(1+\delta_{n,0})\alpha_0^2\tilde{\alpha}_i\tilde{\alpha}_k}{\beta_r r^2} \times \int_\infty e^{-i(\alpha_1\zeta_1+\alpha_2\zeta_2)}\frac{1}{2}\left[e^{-i\alpha_3\zeta_3} + e^{i(\alpha_3\zeta_3+\delta_{3i}\pi+\delta_{3k}\pi)}\right]\left[\left(1 - \frac{\tilde{\xi}^2}{l^2}\right)\delta_{ik} + \frac{\tilde{\xi}_i\tilde{\xi}_k}{l^2}\right]e^{-\tilde{\xi}^2/l^2} M^p_{m,n}(\zeta_1,\zeta_2)d\vec{\xi} \tag{67}$$

where

$$M^p_{m,n} \equiv \frac{\Delta}{4\pi p}\int_{-\infty}^{\infty} \exp\left[-i(\omega + \alpha_1 U_c)\tau - \omega_f|\tau| - \left(\frac{\beta_r}{\beta^2}\right)|\zeta_1 + U_c\tau|\frac{2\pi p}{\Delta}\right]\cos\left\{\frac{2\pi p}{\Delta}\left[\frac{MM_t}{\beta^2}(U_c\tau + \zeta_1) + \zeta_2 + U_t\tau\right]\right\}d\tau \tag{68}$$

$$\tilde{\alpha}_i = \begin{cases} r\alpha_i & \text{for } i = 1 \\ \alpha_i & \text{for } i \neq 1 \end{cases} \tag{69}$$

Equation (67) can be written as

$$\Omega^p_{m,n} = \lim_{\lambda \to 1} \frac{2\pi\rho_0^2 \delta b U_t^2 u_1^2 \theta^2 (1 + \delta_{n,0}) \alpha_0^2}{\beta_r r^2} \left[ -\frac{1}{l^2} \frac{\partial^2}{\partial \lambda^2} + \tilde{\alpha}^2 \left( 1 - \frac{l}{2} \frac{\partial}{\partial l} \right) \right]$$

$$\times \int e^{-i(\alpha_1 \zeta_1 + \alpha_2 \zeta_2)\lambda} \frac{1}{2} \left( e^{-i\alpha_3 \zeta_3 \lambda} + e^{i\alpha_3 \lambda \zeta_3} \right) e^{-\tilde{\zeta}^2 / l^2} M^p_{m,n} d\vec{\zeta}$$

where

$$\tilde{\alpha}^2 = r^2 \alpha_1^2 + \alpha_2^2 + \alpha_3^2 \tag{70}$$

Upon carrying out the integration with respect to $\zeta_3$, this becomes

$$\Omega^p_{m,n} = \frac{2\pi\rho_0^2 \delta b U_t^2 \overline{u_1^2} \theta^2 (1 + \delta_{n,0}) \alpha_0^2}{\beta_r r^2} \sqrt{\pi} \lim_{\lambda \to 1} \left[ -\frac{1}{l^2} \frac{\partial^2}{\partial \lambda^2} + \tilde{\alpha}^2 \left( 1 - \frac{l}{2} \frac{\partial}{\partial l} \right) \right] l \, e^{-(\alpha_3 \lambda l / 2)^2}$$

$$\times \int_{-\infty}^{\infty} \int \exp \left[ -i(\alpha_2 \zeta_2 + \alpha_1 \zeta_1)\lambda - \left( \frac{\zeta_2}{l} \right)^2 - \left( \frac{\zeta_1}{rl} \right)^2 \right] M^p_{m,n} \, d\zeta_1 \, d\zeta_2 \tag{71}$$

It is shown in appendix A that

$$M^p_{m,n} = -\frac{1}{2} \left[ e^{(2\pi p/\Delta) i \zeta_2} K^+_{m,n,p}(\zeta_1) + e^{-(2\pi p/\Delta) i \zeta_2} K^-_{m,n,p}(\zeta_1) \right]$$

where $K^{\pm}_{m,n,p}$ are given by equation (A2). Inserting this into equation (71) and carrying out the integration over $\zeta_2$ shows that

$$\Omega^{p}_{m,n} = -\frac{\pi^2\rho_0^2\delta b U_t^2 \overline{u_1^2}\theta^2(1+\delta_{n,0})}{\beta_r r^2}\,\alpha_0^2 \lim_{\lambda\to 1}\left[-\frac{1}{l^2}\frac{\partial^2}{\partial\lambda^2} + \tilde{\alpha}^2\left(1-\frac{l}{2}\frac{\partial}{\partial l}\right)\right] l^2 e^{-(\alpha_3\lambda l/2)^2}$$

$$\times\left[e^{-l^2(\alpha_2\lambda - 2\pi p/\Delta)^2/4}\int e^{-(\xi_1/rl)^2 - i\alpha_1\xi_1\lambda}\,K^{+}_{m,n,p}\,d\xi_1\right.$$

$$\left. + e^{-l^2(\alpha_2\lambda + 2\pi p/\Delta)^2/4}\int e^{-(\xi_1/rl)^2 - i\alpha_1\xi_1\lambda}\,K^{-}_{m,n,p}\,d\xi_1\right] \qquad (72)$$

But

$$\int e^{-\xi_1^2/r^2l^2 - i\alpha_1\lambda\xi_1}\,K^{+}_{m,n,p}\,d\xi_1$$

$$= \frac{\sqrt{\pi}}{2}\,lr\left[\frac{\left(\frac{\omega_f\Delta}{2\pi p}\right)\exp\left\{\frac{r^2l^2\left[\left(\frac{2\pi p}{\Delta}\right)D - i\alpha_1\lambda\right]^2}{4}\right\}\operatorname{erfc}\frac{rl}{2}\left(\frac{2\pi p}{\Delta}D - i\alpha_1\lambda\right)}{\left[\frac{2\pi p}{\Delta}DU_c - i\,\omega + \alpha_1 U_c - \frac{2\pi p}{\Delta}U_t\right)\right]^2 - \omega_f^2}\right.$$

$$+\frac{\left(\frac{\beta_r U_c}{\beta^2}\right)\exp\left(\frac{r^2l^2\left\{\omega_f + i\left[\omega + \alpha_1(1-\lambda)U_c - \frac{2\pi pU_t}{\Delta}\right]\right\}^2}{4U_c^2}\right)}{\left\{\omega_f + i\left[\omega + \alpha_1 U_c - \frac{2\pi p}{\Delta}\left(1 + \frac{MM_c}{\beta^2}\right)U_t\right]\right\}^2 - \left(\frac{2\pi p}{\Delta}\frac{\beta_r}{\beta^2}U_c\right)^2}$$

$$\left.\times\operatorname{erfc}\frac{lr}{2U_c}\left\{\omega_f + i\left[\omega + \alpha_1(1-\lambda)U_c - \frac{2\pi pU_t}{\Delta}\right]\right\} + \text{c. c.}\right]$$

where c. c. denotes the complrex conjugate of the preceding expression. A similar expression holds for the integral over $K^{-}_{m,n,p}$. It can be obtained from the preceding equation by replacing p by -p. Hence, equation (72) can be written as

$$\Omega^{p}_{m,n} = -\frac{\pi^2 \rho_0^2 \delta b U_t^2 \overline{u_1^2} \theta^2 \sqrt{\pi}(1+\delta_{n,0})}{c_0 \beta_r r} \alpha_0^2$$

$$\times \lim_{\lambda \to 1} \left[ -\frac{1}{l^2} \frac{\partial^2}{\partial \lambda^2} + \tilde{\alpha}^2 \left(1 - \frac{l}{2} \frac{\partial}{\partial l}\right) \right] l^3 e^{-(\alpha_3 \lambda l/2)^2} \; Re\left\{\Gamma^{p}_{m,n} + \Gamma^{-p}_{m,n}\right\} \tag{73}$$

where

$$\Gamma^{p}_{m,n} = \left\{ \exp\left[ \frac{-l^2 \left(\frac{2m\pi\lambda}{\delta} - \frac{2\pi p}{\Delta}\right)^2}{4} \right] \right\} \times \left\{ \frac{\left(\frac{c_0 \omega_f \Delta}{2\pi p}\right) W\left[\frac{il\,r}{2}\left(\frac{2\pi p}{\Delta} D - i\alpha_1 \lambda\right) \operatorname{sgn} p\right]}{\left[\frac{2\pi p}{\Delta} D U_c - i\left(\omega + \alpha_1 U_c - \frac{2\pi p}{\Delta} U_t\right)\right]^2 - \omega_f^2} \right.$$

$$\left. + \frac{\left(\frac{c_0 \beta_r U_c}{\beta^2}\right) W\left(\frac{il\,r}{2U_c}\left\{\omega_f + i\left[\omega + \alpha_1(1-\lambda)U_c - \frac{2\pi p U_t}{\Delta}\right]\right\}\right)}{\left\{\omega_f + i\left[\omega + \alpha_1 U_c - \frac{2\pi p}{\Delta} U_t\left(1 + \frac{MM_c}{\beta^2}\right)\right]\right\}^2 - \left(\frac{2\pi p}{\Delta} \frac{\beta_r}{\beta^2} U_c\right)^2} \right\} \tag{74}$$

where $\alpha_1$ is the same as $\alpha_1^+$ defined by equation (17), W(Z) is defined in reference 9 by

$$W(Z) \equiv e^{-Z^2} \operatorname{erfc}(iZ)$$

and

$$\operatorname{sgn}(x) = \begin{cases} 1 & \text{if } x > 0 \\ -1 & \text{if } x < 0 \end{cases}$$

## Derivation of Final Sound Power Equation

Substituting equation (73) into equation (23) (with the upper sign) and using equations (17) and (58) show that

$$\mathcal{P}^+(\omega) = \frac{\rho_0 U_t^2 \overline{u_1^2} \theta^2 \sqrt{\pi}}{4 c_0^2 \beta_r r} \sum_{\substack{\text{All m and} \\ n \geq 0 \text{ with} \\ k^2 > \beta^2 \kappa_{m,n}^2}} \frac{1 + A_{m,n}^2 - (M - M_t A_{m,n})^2}{k_{m,n}}$$

$$\times \lim_{\lambda \to 1} \left[ -\frac{1}{\ell^2} \frac{\partial^2}{\partial \lambda^2} + \tilde{\alpha}^2 \left( 1 - \frac{\ell}{2} \frac{\partial}{\partial \ell} \right) \right] \ell^3 e^{-(n\pi\lambda\ell/2b)^2} \sum_{\substack{p=-\infty \\ p \neq 0}}^{\infty} \Gamma_{m,n}^p \qquad (75)$$

where $\Gamma_{m,n}^p$ is given by equation (74)

$$A_{m,n} \equiv \frac{\frac{2m\pi\beta}{\delta}}{Mk + k_{m,n}} \qquad (76)$$

and equations (17) and (70) show that

$$\tilde{\alpha}^2 = \frac{r^2}{\beta^2} (Mk + k_{m,n})^2 + \left( \frac{2m\pi}{\delta} \right)^2 + \left( \frac{n\pi}{b} \right)^2 \qquad (77)$$

## DISCUSSION OF RESULTS

Equations (74) to (77) are the final results. They can be used to calculate the power spectral density of the quadrupole sound emitted by a fan as a result of inlet turbulence. In order to do this, it is necessary to specify the longitudinal correlation length $\ell$ of the turbulence in the direction transverse to the flow, the ratio $r$ of the longitudinal correlation length in the axial direction to the transverse longitudinal correlation length, the mean square turbulence velocity $\overline{u_1^2}$, the turbulence convection velocity $U_c$, and the characteristic frequency $\omega_f$ of the moving-frame correlation. The parameters b, B, $\Delta$, and $\delta = B\Delta$ characterize the geometry of the fan. The remaining parameters depend on the operating conditions of the fan. They are the tip speed $U_t$, the through-flow (axial) velocity U, and the work coefficient $\theta$. The work coefficient is a measure of the loading on the fan.

In most high-Reynolds-number turbulent flows the characteristic frequency $\omega_f$ of the moving-frame turbulence correlation tensor is quite small compared with the frequency $U_c/l$ of the turbulence observed in a fixed frame (Taylor's hypothesis). In this case we can set $\omega_f$ equal to zero and the first term in equation (74) vanishes. Since the second term is only weakly dependent on $\omega_f$, it can be associated with noise generated by the time unsteadiness of the turbulence. The second term therefore represents the generation of noise by the spatial nonuniformities and the convection of these nonuniformities by the mean flow. With $\omega_f$ equal to zero, equation (74) becomes

$$\Gamma^p_{m,n} = -\frac{c_0\beta_r U_c}{\beta^2} \exp\left[\frac{-l^2\left(\frac{2m\pi\lambda}{\delta} - \frac{2\pi p}{\Delta}\right)^2}{4}\right] \frac{W\left\{-\frac{lr}{2U_c}\left[\omega + \alpha_1(1-\lambda)U_c - \frac{2\pi p U_t}{\Delta}\right]\right\}}{\left[\omega + \alpha_1 U_c - \frac{2\pi p}{\Delta} U_t\left(1+\frac{MM_c}{\beta^2}\right)\right]^2 + \left(\frac{2\pi p}{\Delta}\frac{\beta_r}{\beta^2} U_c\right)^2} \tag{78}$$

The function $W(Z/\sigma)$ of $Z$ exhibits a peak at $Z = 0$ whose width is equal to $2\sigma$. Hence, it follows from equation (78) (with $\lambda = 1$) and equation (75) that the spectrum will exhibit peaks at frequencies

$$\omega = 2\pi p \frac{U_t}{\Delta} = 2\pi pB \frac{U_t}{\delta} = pB\Omega \qquad \text{for } p = 1, 2, \ldots$$

where $\Omega \equiv 2\pi U_t/\delta$ is the angular velocity of the rotor. Thus, equation (75) does indeed predict tone production at the multiple of the blade passing frequency. It can also be seen that the width of the tone is $4U_c/lr$. The convection velocities of the eddies are probably nearly equal to the axial flow velocity U, which for most of the Quiet Fans is nearly equal to one-half the speed of sound. Typical fan spectra measured at Lewis exhibit tones which are of the order of 100 to 200 hertz in width. Hence, the turbulent eddies must be of the order of 1 to 2 feet in length in order to produce such tones. Since the most intense turbulence entering the fan is in the casing boundary layer, whose width is considerably less than this, it is fairly unlikely that the turbulence is producing the tones unless an extremely large amount of stretching of the eddies occurs. Thus, it has been postulated that when a nontranslating fan is operating out doors, large-scale turbulence shed from buildings and nearby structures is drawn into the fan and, due to the large convergence of the mean streamline, the eddies become very elongated in the direction of flow. In any event the turbulence could still contribute to the broad sidebands which are invariably observed in the tones of fan spectra.

In figures 5 to 9, dimensionless acoustic spectra are plotted against dimensionless frequency for various values of the design and turbulence parameters. Since the work coefficient $\theta$ and the turbulence intensity $\sqrt{\overline{u_1^2}/U^2}$ enter equation (75) simply as multiplicative factors, we absorb these into the dimensionless acoustic spectrum. Since, as we have indicated, most of the subsonic Quiet Fans operated at the Lewis Research Center have an axial-flow Mach number of approximately 1/2, all the plots are drawn with $M = 0.45$. It is also reasonable to assume that the convection velocity $U_c$ of the turbulent eddies is equal to the axial-flow velocity U. All figures are drawn for this case. In all plots except figure 9, $\omega_f$ is taken to be equal to $10^{-4}\, c_0/\Delta$. This is essentially equivalent to putting it equal to zero in equation (74) (which amounts to using eq. (78)).

The effect of varying the axial correlation length of the turbulent eddies is illustrated in figure 5. It can be seen from figure 5(a) that when the correlation length $l$ in the transverse direction is as small as one-half the blade gap $\Delta$ and when the ratio r of the axial correlation length to the transverse correlation length is less than 1/2, there is virtually no evidence of tones. It is not at all unreasonable to suppose that much of the turbulence entering a full-size fan (most of which is in the casing boundary layer) is of this size. When either of the turbulence correlation lengths starts to become equal to the blade gap, the spectrum rapidly begins to form humps at the blade passing frequency and its harmonics. These humps are formed chiefly through a decrease in the sound power in the region lying between the harmonics of the blade passing frequency, with the level of the tones remaining relatively constant. The tones are quite broad until the correlation length is of the order of several blade gaps. Figure 5(b) shows that far narrower tones can indeed be produced by eddies which are 10 blade spacings long.

It can also be seen from figure 5 that the power in the tone at the second harmonic of the blade passing frequency is nearly equal to (or in some cases greater than) the power in the fundamental. For most fans tested at Lewis the second harmonic is about 5 decibels lower than the fundamental. This is an indication that inlet turbulence may not be the chief producer of tones in these fans (at least through the quadrupole mechanism).

The effect on the acoustic spectrum of varying the blade rotational Mach number $M_t$ is illustrated in figure 6. It can be seen from figure 6(b) that when the eddies are small, increasing $M_t$ tends to increase the power radiated in the tones while leaving that radiated at intermediate frequencies unchanged. There also appears to be a tendency to shift the spectrum to higher frequencies as $M_t$ increases.

In figure 7 the effect of varying the blade number B is shown, while figure 8 shows the effect of varying the blade height b. It can be seen from these figures that there is very little change in the shape of the spectra as these parameters vary and that doubling B or b roughly doubles (i. e., increases by 3 dB) the sound power radiated at each frequency. But the cross-sectional area of the fan is proportional to $B \times b$. Hence, the

power radiated per unit cross-sectional area of the fan remains roughly unchanged as B or b is varied. This tendency is observed in the Quiet Fans tested at Lewis.

Finally, figure 9 shows the effect of varying the moving-frame turbulence frequency $\omega_f$. In most cases which occur in practice, $\omega_f \Delta / c_0$ will be very nearly zero, and the value of $10^{-1}$ used in figure 9 is much too large. However, this large value was chosen so that the effect of this parameter will show up. It can be seen that increasing $\omega_f$ merely fills in the spectrum between the tones.

## CONCLUDING REMARKS

Inlet turbulence can be a dominant source of fan noise and at the high subsonic Mach number where current aircraft engine fans operate, it is quite possible that this noise is being generated through a quadrupole mechanism. But, for the high-subsonic-Mach-number regime, no quadrupole analysis of this noise source has been developed. The present report is written to fill this gap. The numerical results exhibit a number of features observed in actual fan spectra. However, they also show that, unless the turbulent eddies become extremely elongated as they enter the inlet of the fan, this mechanism contributes mainly to the broadband noise spectrum. But there increasing evidence that such elongation does indeed occur when the fan is not translating and that as a result inlet turbulence is the dominant source of the pure tones. The present results may be helpful in resolving this question.

Lewis Research Center,
National Aeronautics and Space Administration,
Cleveland, Ohio, March 7, 1974,
501-04.

## APPENDIX A

## EVALUATION OF $M^{p}_{m,n}$

For $\zeta_1 < 0$ equation (68) becomes

$$
\begin{aligned}
M^{p}_{m,n} = \frac{1}{2}\frac{\Delta}{4\pi p}\Bigg\{ & \int_{-\infty}^{0} \exp\left\{-\left[i(\omega + \alpha_1 U_c) - \omega_f - \left(\frac{2\pi p}{\Delta}\right)\left(\frac{\beta_r}{\beta^2}\right)U_c\right]\tau\right\}\left\{\exp\left[\left(\frac{2\pi p}{\Delta}\right)\left(\frac{\beta_r}{\beta^2}\right)\zeta_1\right]\right\} \\
& \times \left(\exp\left\{\left(\frac{2\pi i p}{\Delta}\right)\left[(\zeta_2 + U_t\tau) + \left(\frac{MM_t}{\beta^2}\right)(U_c\tau + \zeta_1)\right]\right\} + \exp\left\{-\left(\frac{2\pi i p}{\Delta}\right)\left[(\zeta_2 + U_t\tau) + \left(\frac{MM_t}{\beta^2}\right)(U_c\tau + \zeta_1)\right]\right\}\right)d\tau \\
& + \int_{0}^{-\zeta_1/U_c} \exp\left\{-\left[i(\omega + \alpha_1 U_c) + \omega_f - \left(\frac{2\pi p}{\Delta}\right)\left(\frac{\beta_r}{\beta^2}\right)U_c\right]\tau\right\}\exp\left[\left(\frac{2\pi p}{\Delta}\right)\left(\frac{\beta_r}{\beta^2}\right)\zeta_1\right] \\
& \times \left(\exp\left\{\left(\frac{2\pi p}{\Delta}\right)i\left[(\zeta_2 + U_t\tau) + \left(\frac{MM_t}{\beta^2}\right)(U_c\tau + \zeta_1)\right]\right\} + \exp\left\{-\left(\frac{2\pi p}{\Delta}\right)i\left[(\zeta_2 + U_t\tau) + \left(\frac{MM_t}{\beta^2}\right)(U_c\tau + \zeta_1)\right]\right\}\right)d\tau \\
& + \int_{-\zeta_1/U_c}^{\infty} \exp\left\{-\left[i(\omega + \alpha_1 U_c) + \omega_f + \left(\frac{2\pi p}{\Delta}\right)\left(\frac{\beta_r}{\beta^2}\right)U_c\right]\tau\right\}\exp\left[-\left(\frac{2\pi p}{\Delta}\right)\left(\frac{\beta_r}{\beta^2}\right)\zeta_1\right] \\
& \times \left(\exp\left\{\left(\frac{2\pi p}{\Delta}\right)i\left[(\zeta_2 + U_t\tau) + \left(\frac{MM_t}{\beta^2}\right)(U_c\tau + \zeta_1)\right]\right\} + \exp\left\{-\left(\frac{2\pi p}{\Delta}\right)i\left[(\zeta_2 + U_t\tau) + \left(\frac{MM_t}{\beta^2}\right)(U_c\tau + \zeta_1)\right]\right\}\right)d\tau\Bigg\}
\end{aligned}
$$

Upon carrying out the integrations this becomes

$$M^{p}_{m,n} = \frac{1}{2}\frac{\Delta}{4\pi p}\left\{\exp\left[\left(\frac{2\pi p}{\Delta}\right)\left(\frac{\beta_r}{\beta^2}\right)\zeta_1\right]\left(\frac{\exp\left\{\frac{2\pi i p}{\Delta}\left[\zeta_2+\left(\frac{MM_t}{\beta^2}\right)\zeta_1\right]\right\}}{\omega_f+\left(\frac{2\pi p}{\Delta}\right)\left(\frac{\beta_r}{\beta^2}\right)U_c-i\left[\omega+\alpha_1U_c-\frac{2\pi p}{\Delta}\left(U_t+\frac{MM_tU_c}{\beta^2}\right)\right]}+\frac{\exp\left\{-\frac{2\pi i p}{\Delta}\left[\zeta_2+\left(\frac{MM_t}{\beta^2}\right)\zeta_1\right]\right\}}{\omega_f+\left(\frac{2\pi p}{\Delta}\right)\left(\frac{\beta_r}{\beta^2}\right)U_c-i\left[\omega+\alpha_1U_c+\frac{2\pi p}{\Delta}\left(U_t+\frac{MM_tU_c}{\beta^2}\right)\right]}\right.\right.$$

$$\left.-\frac{\exp\left\{\left(\frac{2\pi i p}{\Delta}\right)\left[\zeta_2+\left(\frac{MM_t}{\beta^2}\right)\zeta_1\right]\right\}}{\left(\frac{2\pi p}{\Delta}\right)\left(\frac{\beta_r}{\beta^2}\right)U_c-\omega_f-i\left[\omega+\alpha_1U_c-\frac{2\pi p}{\Delta}\left(U_t+\frac{MM_tU_c}{\beta^2}\right)\right]}-\frac{\exp\left\{-\left(\frac{2\pi i p}{\Delta}\right)\left[\zeta_2+\left(\frac{MM_t}{\beta^2}\right)\zeta_1\right]\right\}}{\left(\frac{2\pi p}{\Delta}\right)\left(\frac{\beta_r}{\beta^2}\right)U_c-\omega_f-i\left[\omega+\alpha_1U_c+\frac{2\pi p}{\Delta}\left(U_t+\frac{MM_tU_c}{\beta^2}\right)\right]}\right)$$

$$+\exp\left\{\left[\omega_f+i(\omega+\alpha_1U_c)\right]\left(\frac{\zeta_1}{U_c}\right)\right\}\left(\frac{\exp\left\{\left(\frac{2\pi i p}{\Delta}\right)\left[\zeta_2-\left(\frac{U_t}{U_c}\right)\zeta_1\right]\right\}}{\left(\frac{2\pi p}{\Delta}\right)\left(\frac{\beta_r}{\beta^2}\right)U_c-\omega_f-i\left[\omega+\alpha_1U_c-\frac{2\pi p}{\Delta}\left(U_t+\frac{MM_tU_c}{\beta^2}\right)\right]}+\frac{\exp\left\{-\left(\frac{2\pi i p}{\Delta}\right)\left[\zeta_2-\left(\frac{U_t}{U_c}\right)\zeta_1\right]\right\}}{\left(\frac{2\pi p}{\Delta}\right)\left(\frac{\beta_r}{\beta^2}\right)U_c-\omega_f-i\left[\omega+\alpha_1U_c+\frac{2\pi p}{\Delta}\left(U_t+\frac{MM_tU_c}{\beta^2}\right)\right]}\right.$$

$$\left.\left.-\frac{\exp\left\{\left(\frac{2\pi i p}{\Delta}\right)\left[\zeta_2-\left(\frac{U_t}{U_c}\right)\zeta_1\right]\right\}}{-\left(\frac{2\pi p}{\Delta}\right)\left(\frac{\beta_r}{\beta^2}\right)U_c-\omega_f-i\left[\omega+\alpha_1U_c-\frac{2\pi p}{\Delta}\left(U_t+\frac{MM_tU_c}{\beta^2}\right)\right]}-\frac{\exp\left\{-\left(\frac{2\pi i p}{\Delta}\right)\left[\zeta_2-\left(\frac{U_t}{U_c}\right)\zeta_1\right]\right\}}{-\left(\frac{2\pi p}{\Delta}\right)\left(\frac{\beta_r}{\beta^2}\right)U_c-\omega_f-i\left[\omega+\alpha_1U_c+\frac{2\pi p}{\Delta}\left(U_t+\frac{MM_tU_c}{\beta^2}\right)\right]}\right)\right\}$$

**Similarly for $\zeta_1 > 0$**

$$M^{p}_{m,n} = \frac{1}{2}\frac{\Delta}{4\pi p}\left\{\exp\left\{\left[i(\omega+\alpha_1U_c)-\omega_f\right]\frac{\zeta_1}{U_c}\right\}\left(\frac{\exp\left\{\left(\frac{2\pi p}{\Delta}\right)i\left[\zeta_2-\left(\frac{U_t}{U_c}\right)\zeta_1\right]\right\}}{\omega_f+\left(\frac{2\pi p}{\Delta}\right)\left(\frac{\beta_r}{\beta^2}\right)U_c-i\left[\omega+\alpha_1U_c-\frac{2\pi p}{\Delta}\left(U_t+\frac{MM_tU_c}{\beta^2}\right)\right]}+\frac{\exp\left\{-\left(\frac{2\pi p}{\Delta}\right)i\left[\zeta_2-\left(\frac{U_t}{U_c}\right)\zeta_1\right]\right\}}{\omega_f+\left(\frac{2\pi p}{\Delta}\right)\left(\frac{\beta_r}{\beta^2}\right)U_c-i\left[\omega+\alpha_1U_c+\frac{2\pi p}{\Delta}\left(U_t+\frac{MM_tU_c}{\beta^2}\right)\right]}\right.\right.$$

$$\left.-\frac{\exp\left\{\left(\frac{2\pi p}{\Delta}\right)i\left[\zeta_2-\left(\frac{U_t}{U_c}\right)\zeta_1\right]\right\}}{\omega_f-\left(\frac{2\pi p}{\Delta}\right)\left(\frac{\beta_r}{\beta^2}\right)U_c-i\left[\omega+\alpha_1U_c-\frac{2\pi p}{\Delta}\left(U_t+\frac{MM_tU_c}{\beta^2}\right)\right]}-\frac{\exp\left\{-\left(\frac{2\pi p}{\Delta}\right)i\left[\zeta_2-\left(\frac{U_t}{U_c}\right)\zeta_1\right]\right\}}{\omega_f-\left(\frac{2\pi p}{\Delta}\right)\frac{\beta_r}{\beta^2}U_c-i\left[\omega+\alpha_1U_c+\frac{2\pi p}{\Delta}\left(U_t+\frac{MM_tU_c}{\beta^2}\right)\right]}\right)$$

$$+\exp\left[-\left(\frac{2\pi p}{\Delta}\right)\left(\frac{\beta_r}{\beta^2}\right)\zeta_1\right]\left(\frac{\exp\left\{\left(\frac{2\pi p}{\Delta}\right)i\left[\zeta_2+\left(\frac{MM_t}{\beta^2}\right)\zeta_1\right]\right\}}{\omega_f-\left(\frac{2\pi p}{\Delta}\right)\left(\frac{\beta_r}{\beta^2}\right)U_c-i\left[\omega+\alpha_1U_c-\frac{2\pi p}{\Delta}\left(U_t+\frac{MM_tU_c}{\beta^2}\right)\right]}+\frac{\exp\left\{-\left(\frac{2\pi p}{\Delta}\right)i\left[\zeta_2+\left(\frac{MM_t}{\beta^2}\right)\zeta_1\right]\right\}}{\omega_f-\left(\frac{2\pi p}{\Delta}\right)\frac{\beta_r}{\beta^2}U_c-i\left[\omega+\alpha_1U_c+\frac{2\pi p}{\Delta}\left(U_t+\frac{MM_tU_c}{\beta^2}\right)\right]}\right.$$

$$\left.\left.-\frac{\exp\left\{\left(\frac{2\pi p}{\Delta}\right)i\left[\zeta_2+\left(\frac{MM_t}{\beta^2}\right)\zeta_1\right]\right\}}{-\omega_f-\left(\frac{2\pi p}{\Delta}\right)\left(\frac{\beta_r}{\beta^2}\right)U_c-i\left[\omega+\alpha_1U_c-\frac{2\pi p}{\Delta}\left(U_t+\frac{MM_tU_c}{\beta^2}\right)\right]}-\frac{\exp\left\{-\left(\frac{2\pi p}{\Delta}\right)i\left[\zeta_2+\left(\frac{MM_t}{\beta^2}\right)\zeta_1\right]\right\}}{-\omega_f-\left(\frac{2\pi p}{\Delta}\right)\left(\frac{\beta_r}{\beta^2}\right)U_c-i\left[\omega+\alpha_1U_c+\frac{2\pi p}{\Delta}\left(U_t+\frac{MM_tU_c}{\beta^2}\right)\right]}\right)\right\}$$

Hence, upon simplifying the results, we find that

$$M^{p}_{m,n}(\zeta_1,\zeta_2) \equiv -\frac{1}{2}\left\{\exp\left[\left(\frac{2\pi p}{\Delta}\right)i\zeta_2\right]K^{+}_{m,n,p}(\zeta_1) + \exp\left[-\left(\frac{2\pi p}{\Delta}\right)i\zeta_2\right]K^{-}_{m,n,p}(\zeta_1)\right\} \tag{A1}$$

where

$$K^{\pm}_{m,n,p} = \begin{cases} \dfrac{\frac{\omega_f\Delta}{2\pi p}\exp\left\{\left(\frac{2\pi p}{\Delta}\right)\left[\zeta_1\left(\frac{\beta_r \pm iMM_t}{\beta^2}\right)\right]\right\}}{\left\{\frac{2\pi p}{\Delta}\frac{\beta_r}{\beta^2}U_c - i\left[\omega + \alpha_1 U_c \mp \frac{2\pi p}{\Delta}U_t\left(1+\frac{MM_c}{\beta^2}\right)\right]\right\}^2 - \omega_f^2} + \dfrac{\frac{\beta_r U_c}{\beta^2}\exp\left(\left\{i\left[\omega + \alpha_1 U_c \mp \left(\frac{2\pi p}{\Delta}\right)U_t\right] + \omega_f\right\}\frac{\zeta_1}{U_c}\right)}{\left\{\omega_f + i\left[\omega + \alpha_1 U_c \mp \frac{2\pi p}{\Delta}\left(1+\frac{MM_c}{\beta^2}\right)\right]\right\}^2 - \left(\frac{2\pi p}{\Delta}\frac{\beta_r}{\beta^2}U_c\right)^2} & \zeta_1 < 0 \\ \dfrac{\frac{\omega_f\Delta}{2\pi p}\exp\left\{-\left(\frac{2\pi p}{\Delta}\right)\left[\zeta_1\left(\frac{\beta_r \mp iMM_t}{\beta^2}\right)\right]\right\}}{\left\{\frac{2\pi p}{\Delta}\frac{\beta_r}{\beta^2}U_c + i\left[\omega + \alpha_1 U_c \mp \frac{2\pi p}{\Delta}U_t\left(1+\frac{MM_c}{\beta^2}\right)\right]\right\}^2 - \omega_f^2} + \dfrac{\frac{\beta_r U_c}{\beta^2}\exp\left(\left\{i\left[\omega + \alpha_1 U_c \mp \left(\frac{2\pi p}{\Delta}\right)U_t\right] - \omega_f\right\}\frac{\zeta_1}{U_c}\right)}{\left\{\omega_f - i\left[\omega + \alpha_1 U_c \mp \frac{2\pi p}{\Delta}\left(1+\frac{MM_c}{\beta^2}\right)\right]\right\}^2 - \left(\frac{2\pi p}{\Delta}\frac{\beta_r}{\beta^2}U_c\right)^2} & \zeta_1 > 0 \end{cases} \tag{A2}$$

## APPENDIX B

## SYMBOLS

| | |
|---|---|
| $A_{m,n}$ | defined by eq. (76) |
| $A_0$ | cross-sectional area of $y_3$ = Constant plane |
| B | number of blades |
| b | blade height |
| $C_{m,n}$ | defined by eq. (18) |
| $c_0$ | speed of sound |
| D | $(\beta_r + iMM_2)/\beta^2$ |
| $e_{ij}$ | viscous stress tensor |
| f | function of t or turbulence generating function |
| G | Green's function |
| $H_{jl}, H_j, H'_j$ | rotor velocity integrals, eqs. (35) and (36) |
| $\bar{I}_\omega$ | axial component of acoustic intensity spectrum |
| $\mathcal{I}m$ | imaginary part |
| i | $\sqrt{-1}$ |
| k | wave number, $\omega/c_0$ |
| $k_{m,n}$ | propagation constant, $\sqrt{k^2 - \beta^2\kappa^2_{m,n}}$ |
| $L_{jl}$ | rotor velocity correlations, defined in eq. (51) |
| $l$ | turbulence correlation length in direction transverse to flow |
| M | axial Mach number, $U/c_0$ |
| $M_t$ | rotor tip Mach number, $U_t/c_0$ |
| $M^p_{m,n}$ | defined by eq. (68) |
| n | normal direction to wall |
| $P(\omega)$ | sound pressure spectrum |
| $P^{\pm}_{m,n}(\omega)$ | modes contributing to pressure spectrum |
| $\mathcal{P}^{\pm}(\omega)$ | power spectrum |
| p | pressure measured above ambient pressure |

| | |
|---|---|
| $p_0$ | ambient pressure |
| $\overline{R}$ | mean radius of annular duct |
| $R_{ijk\ell}$, $R_{ij,k}$ $R_{i,jk}$, $R_{ij}$ | turbulence correlation tensors |
| $\mathscr{R}_{ijk\ell}$ | total velocity correlation |
| $\mathscr{R}_{ik}$ | moving-frame turbulence correlation tensor |
| $\mathscr{R}^0_{ik}$ | spatial part of moving-frame turbulence correlation tensor |
| $\mathscr{R}e$ | real part |
| r | ratio of correlation length in axial direction to correlation length in transverse direction |
| S | duct surface |
| T | large time interval |
| $T^\dagger_{ij}$ | Lighthill's stress tensor relative to moving frame |
| t | time (observer) |
| U | axial velocity of flow entering fan |
| $U_c$ | eddy convection velocity |
| $U_r$ | relative velocity, $\sqrt{U_t^2 + U^2}$ |
| $U_t$ | rotor blade-row velocity |
| $u_i$ | turbulence velocity |
| $\overline{u_1^2}$ | mean square axial turbulence velocity |
| V | spectrum of axial acoustic velocity, $v_1^\dagger$ |
| $V_i$ | rotor velocity components relative to blade |
| $v_i$ | fluid velocity, acoustic velocity, $i = 1, 2, 3$ |
| $v_0$ | constant reference velocity (complex) |
| $v_i^\dagger$ | $v_i - \delta_{1i}U$ |
| W(z) | $e^{-z^2}\,\mathrm{erfc}(-iz)$ |
| $w_j$ | phase-locked rotor velocity field |
| $\vec{X}, X_i$ | coordinate system fixed to blades |

| | |
|---|---|
| $x_i, \vec{x}$ | coordinates of observation point |
| $\vec{Y}$ | $\{\eta_1, \eta_2, (\eta_3' + \eta_3)/2\}$ |
| $\vec{y}, y_i$ | coordinates of source point |
| $Z$ | $X_1 + i\beta_r X_2$ |
| $z$ | $\eta_1 D + i\eta_2$ |
| $\alpha_i$ | same as $\alpha_1^+$ |
| $\alpha_i^\pm$ | defined by eq. (17), i = 1, 2, 3 |
| $\alpha_0^2$ | defined by eq. (58) |
| $\tilde{\alpha}^2$ | defined by eq. (70) |
| $\tilde{\alpha}_i$ | defined by eq. (69), i = 1, 2, 3 |
| $\beta$ | $\sqrt{1 - M^2}$ |
| $\beta_r$ | $\sqrt{1 - (U_r/c_0)^2}$ |
| $\Gamma_{m,n}$ | inner product of duct eigenfunctions |
| $\Gamma^p_{m,n}$ | defined by eq. (74) |
| $\Gamma_0$ | circulation |
| $\gamma$ | stagger angle |
| $\Delta$ | interblade spacing |
| $\Delta_0$ | defined by eq. (40) |
| $\delta$ | transverse duct length, $B\Delta$ |
| $\delta_{ij}$ | Kronecker delta |
| $\delta(x)$ | delta function |
| $\zeta_i, \vec{\zeta}$ | turbulence moving-frame coordinates |
| $\eta_i, \vec{\eta}, \eta_i', \vec{\eta}'$ | rotor-locked coordinate system |
| $\theta$ | work coefficient of rotor, $-\Delta w_2/U_t$ |
| $\kappa_{m,n}$ | eigenfunction for transverse modes defined in eq. (9) |
| $\lambda$ | parameter which approaches unity |
| $\lambda_{m,n}$ | defined by eq. (22) |
| $\nu(\tau)$ | region of duct external to blades |

$\vec{\xi}, \xi_i$ separation coordinate $\vec{\eta}' - \vec{\eta}$

$\rho'$ acoustic density fluctuation

$\rho_0$ average density

$\tau$ time (source)

$\Phi_{m,n}$ duct eigenfunctions

$\Omega$ shaft rotational frequency, $2\pi U_t/\delta$

$\Omega^{\dagger}_{m,n}$ defined by eq. (24)

$\Omega^{p}_{m,n}$ defined by eq. (57)

$\omega$ frequency

$\omega_f$ characteristic frequency of turbulence

Subscripts:

i integer 1, 2, 3

j integer 1, 2, 3

k integer 1, 2, 3

$l$ integer 1, 2, 3

m integer 0, ±1, ±2, . . .

n integer 0, 1, 2, . . .

p integer ±1, ±2, . . .

q integer ±1, ±2, . . .

Superscripts:

$\bar{(\,)}$ complex conjugate or time average

† measured relative to a coordinate system moving with flow

## REFERENCES


1. Anon: "Sound Radiation from a Subsonic Rotor Subjected to Turbulence." Proc. Int. Symp. on Fluid Mechanics and Design of Turbomachinery. NASA SP-304, 1974.

2. Mani, R.: Noise Due to Interaction of Inlet Turbulence with Isolated Stators and Rotors. Jour. Sound and Vib., vol. 17, no. 2, July 1971, pp. 251-260.

3. Ffowcs-Williams, J. E.; and Hawkings, D. L.: Theory Relating to the Noise of Rotating Machinery. Jour. Sound and Vib., vol. 10, no. 1, July 1969, pp. 10-21.

4. Chandrashekara, N.: Sound Radiation from Inflow Turbulence In Axial Flow Fans. Jour. Sound and Vib., vol. 19, no. 2, Nov. 1971, pp. 133-146.

5. Cumpsty, N. A.; and Lowrie B. W.: The Cause of Tone Generations by Aeroengine Fans at High Subsonic Tip Speeds and the Effect of Forward Speed. Paper 73-WA/GT-4, ASME, Nov. 1973.

6. Goldstein, Marvin E.: Aeroacoustics. NASA SP-346, 1974, section 4.3.1.

7. Lighthill, M. J.: On Sound Generated Aerodynamically. I. General Theory. Proc. Roy. Soc., vol. 211A, no. 1107, Mar. 20, 1952, pp. 564-587.

8. Abramowitz, Milton, and Stegun, Irlne A., eds. Handbook of Mathematical Functions. With Formulas, Graphs, and Mathematical Tables. National Bureau of Standard Applied Mathematics, Series 55, 1964.

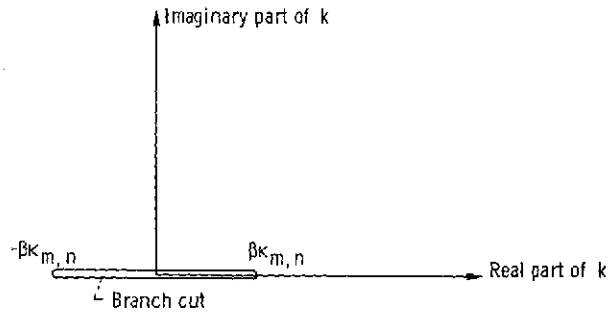


Figure 1. - Branch cut for $\sqrt{k^2 - \beta^2\kappa_{m,n}^2}$.

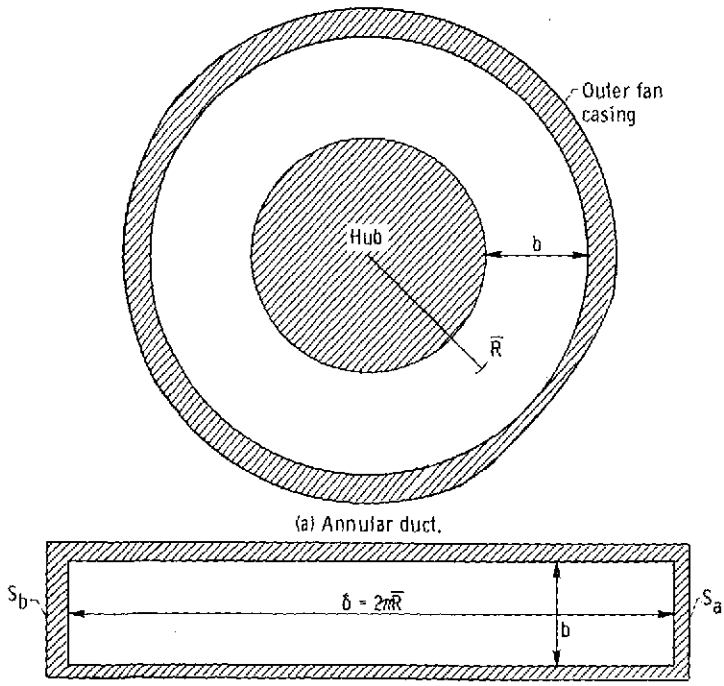


(a) Annular duct.

(b) Annular duct unrolled - rectangular duct.

Figure 2. - Duct cross section.

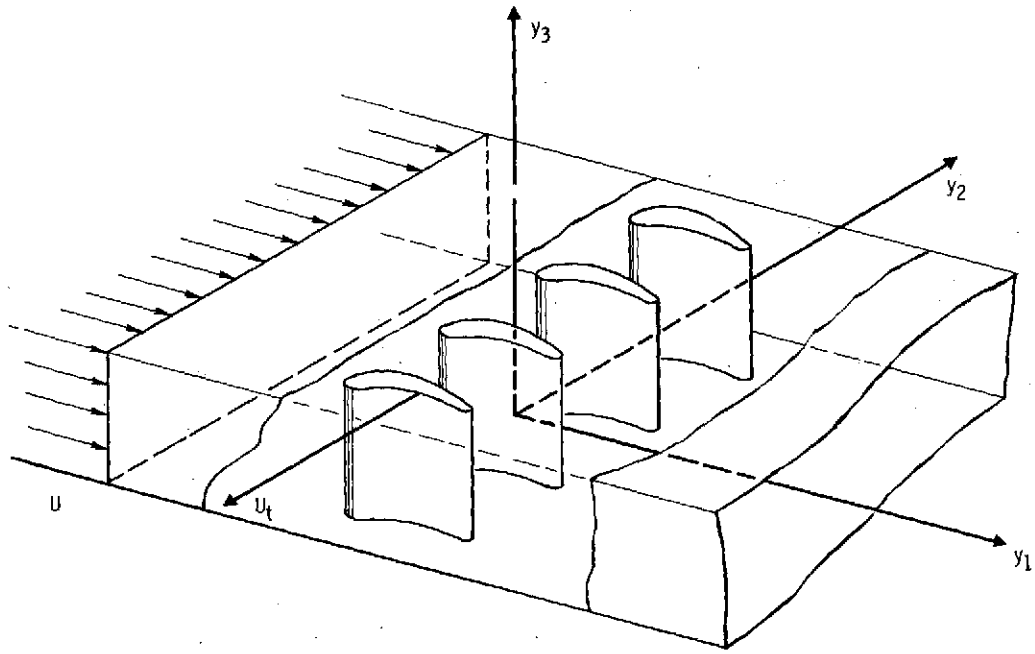


Figure 3. - Configuration of fan in rectangular geometry.

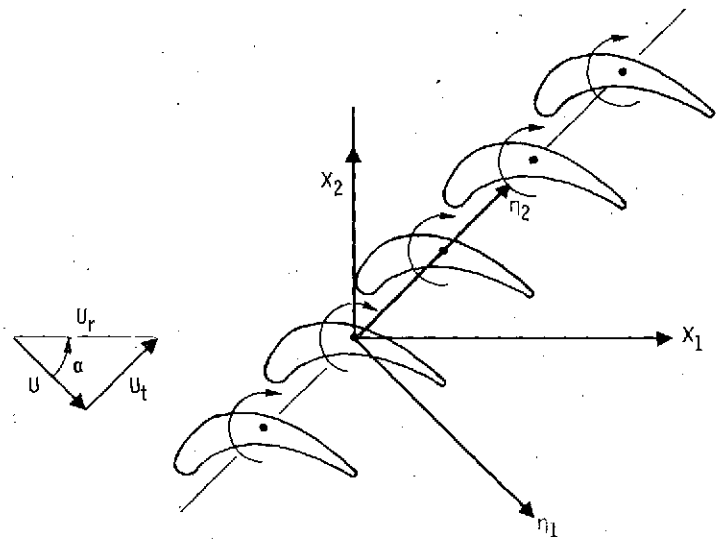


Figure 4. - Blade-oriented coordinate system.

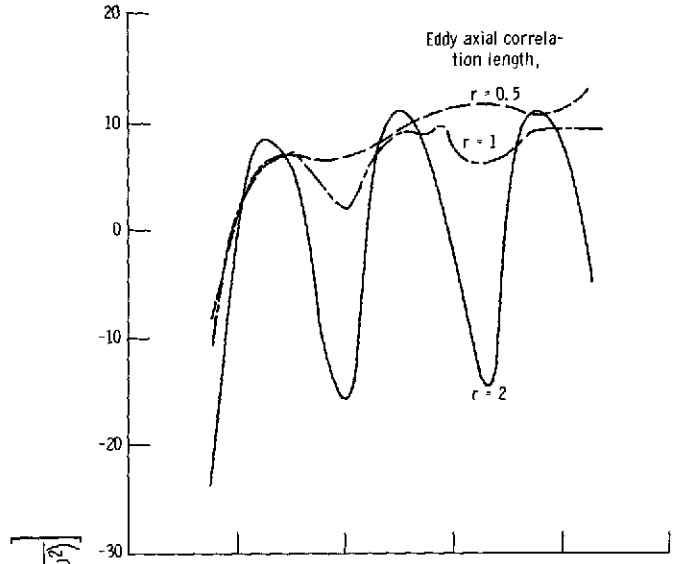


(a) Turbulence correlation length in direction transverse to flow equal to one-half interblade spacing, $\ell = 1/2\,\Delta$.

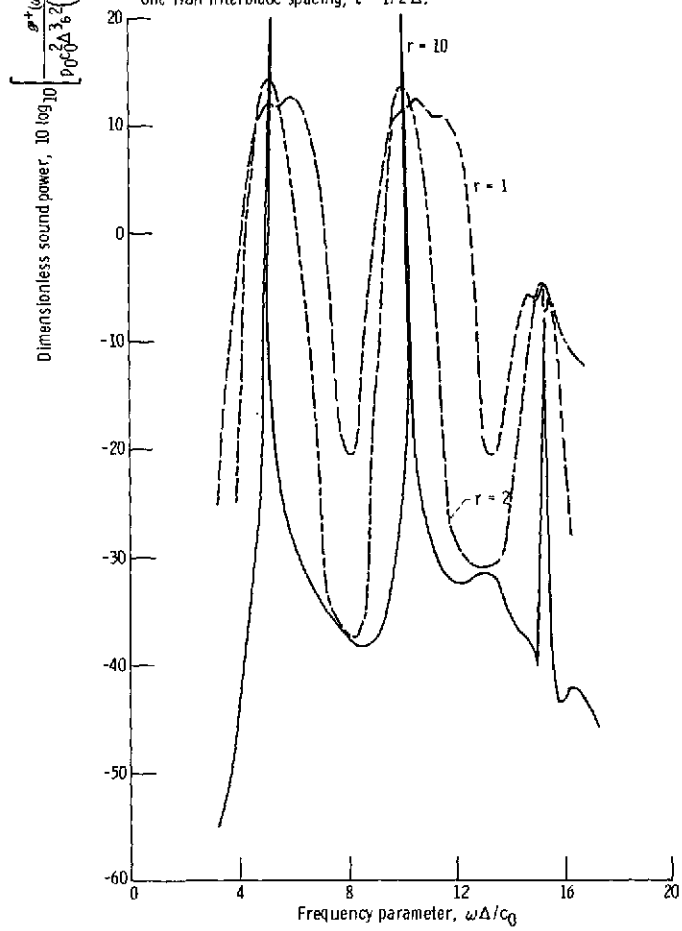


Dimensionless sound power, $10 \log_{10}\left[\frac{\mathscr{P}^{+}(\omega)}{\rho_0^2 \Delta^2 3_b^2 \overline{(u_1^2)(v^2)}}\right]$

(b) Turbulence correlation length in direction transverse to flow equal to interblade spacing, $\ell = \Delta$.

Figure 5. - Effect of eddy axial correlation length on acoustic spectra. Number of blades, B, 30; ratio of blade height to interblade spacing, $b/\Delta$, 4; axial Mach number, M, 0.45; rotor Mach number, $M_t$, 0.8; turbulence frequency parameter, $\omega_1\Delta/c_0$, $10^{-4}$.

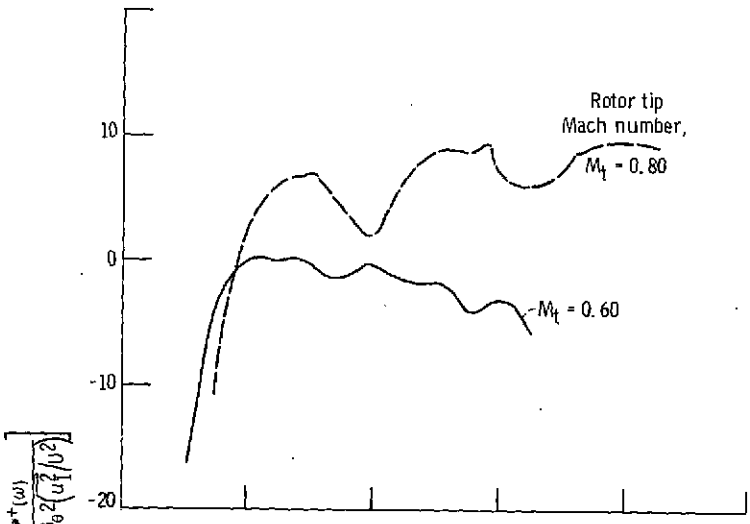


(a) Turbulence correlation length in direction transverse to flow equal to one-half interblade spacing, $\ell = 1/2\ \Delta$.

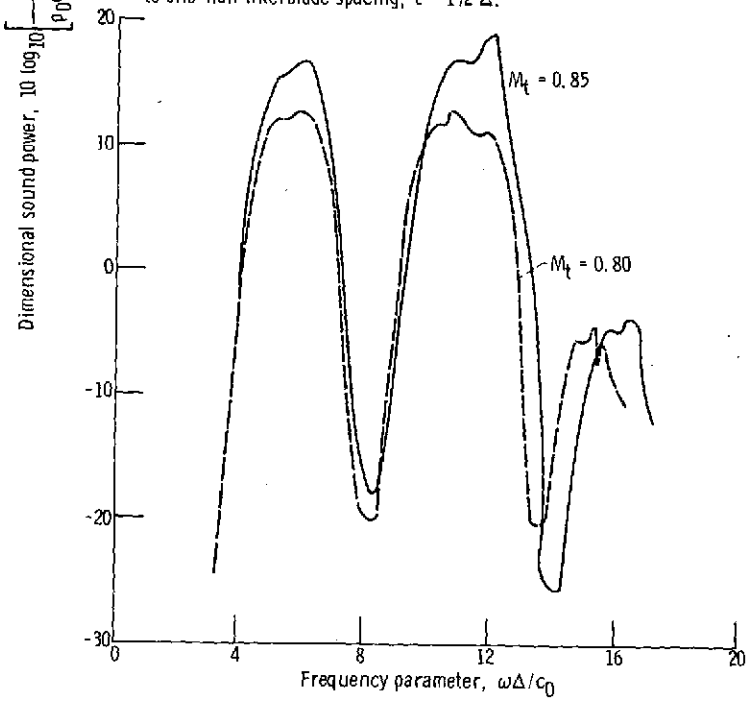


(b) Turbulence correlation length in direction transverse to flow equal to interblade spacing, $\ell = \Delta$.

Figure 6. - Effect of rotor tip Mach number on acoustic spectra. Number of blades, B, 30; ratio of blade height to interblade spacing, $b/\Delta$, 4; axial Mach number, $M_t$, 0.45; eddy correlation length ratio, r, 1; turbulence frequency parameter, $\omega_t\Delta/c_0$, $10^{-4}$

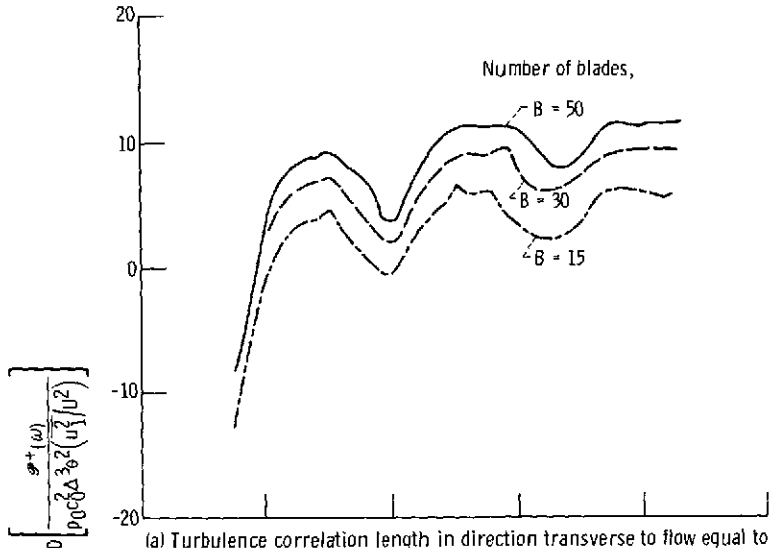


(a) Turbulence correlation length in direction transverse to flow equal to one-half interblade spacing, $\ell = 1/2\,\Delta$.

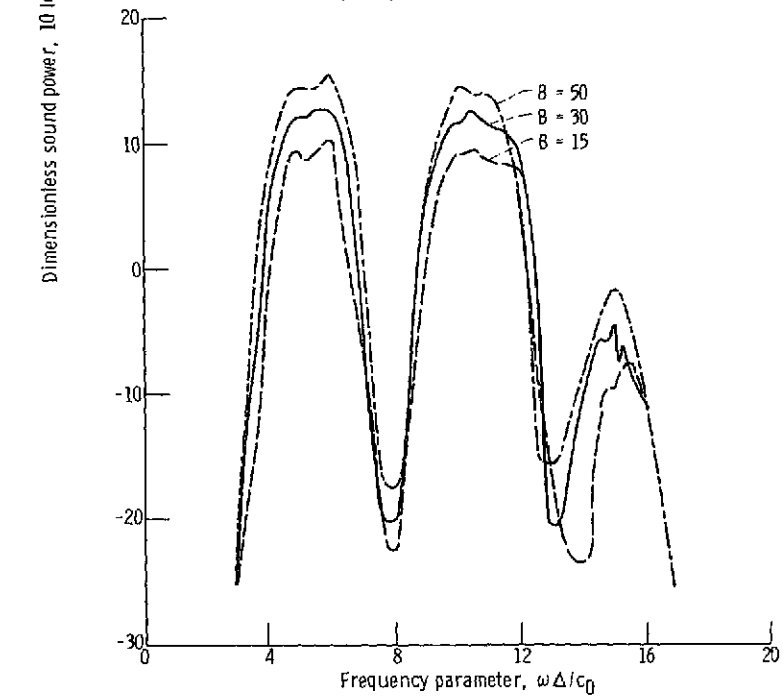


Dimensionless sound power, $10 \log_{10}\left[\frac{\mathcal{P}^+(\omega)}{\rho_0 c_0^3 \Delta^2 \overline{(u_1^2/U^2)}}\right]$

(b) Turbulence correlation length in direction transverse to flow equal to interblade spacing, $\ell = \Delta$.

Figure 7. - Effect of blade number on acoustic spectra. Ratio of blade height to interblade spacing, $b/\Delta$, 4; axial Mach number, M, 0.45; rotor Mach number, $M_t$, 0.8; eddy correlation length ratio, r, 1; turbulence frequency parameter, $\omega_f\Delta/c_0$, $10^{-4}$.

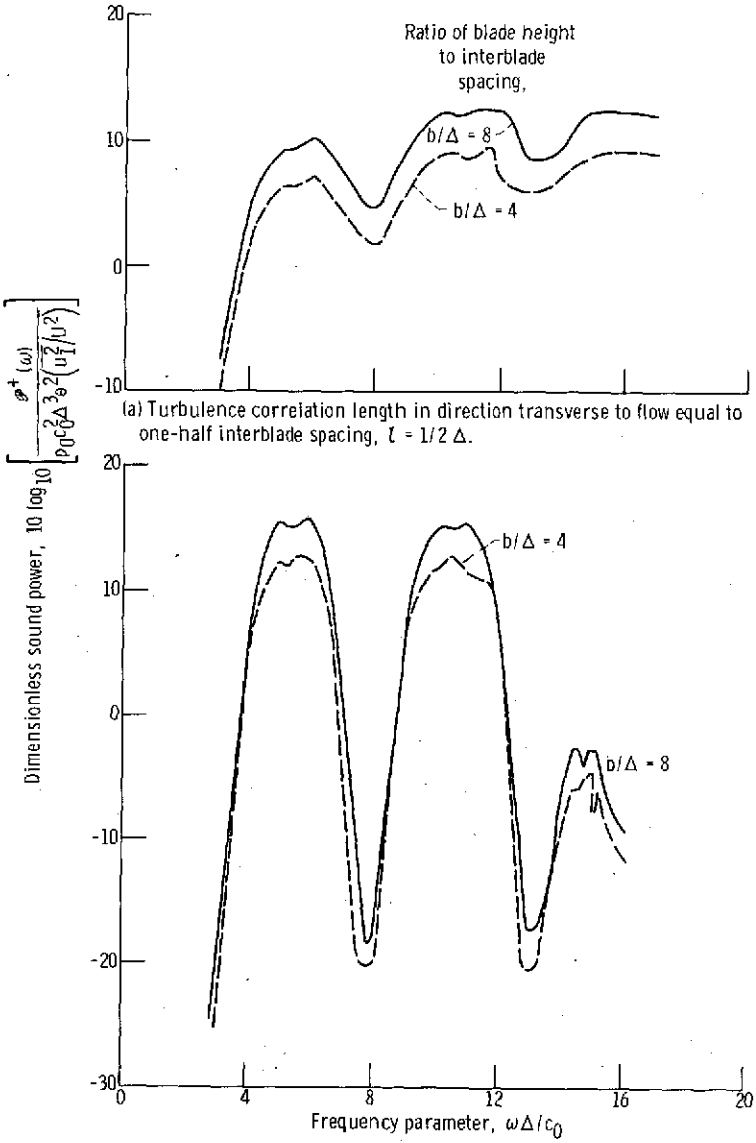


(a) Turbulence correlation length in direction transverse to flow equal to one-half interblade spacing, $\ell = 1/2\,\Delta$.

(b) Turbulence correlation length in direction transverse to flow equal to interblade spacing, $\ell = \Delta$.

Figure 8. - Effect of blade height on acoustic spectra. Number of blades, B, 30; axial Mach number, M, 0.45; rotor Mach number, 0.8; eddy correlation length ratio, r, 1; turbulence frequency parameter, $\omega_t \Delta/c_0$, $10^{-4}$.

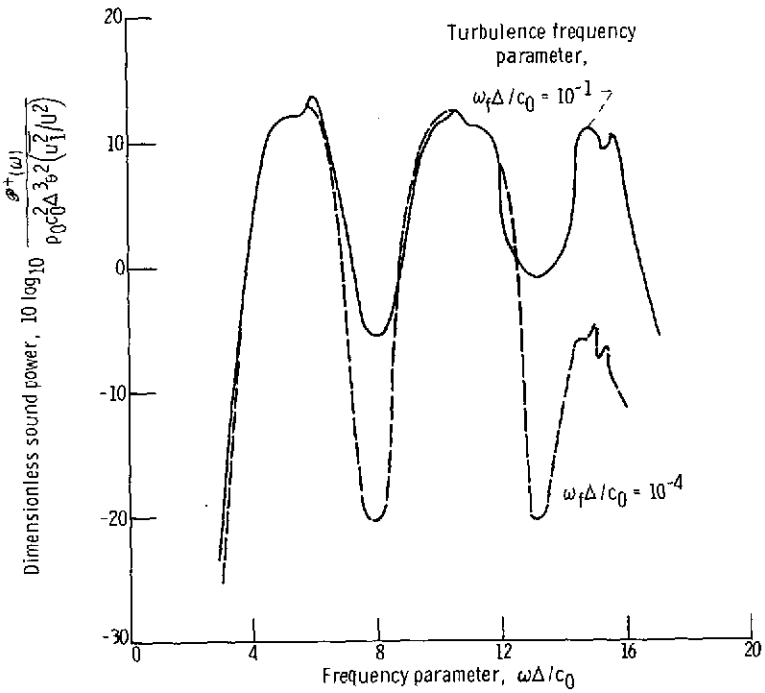


Figure 9. - Effect of turbulence frequency (moving frame) on acoustic spectra. Number of blades, B, 30; ratio of blade height to interblade spacing, $b/\Delta$, 4; axial Mach number, M, 0.45; rotor Mach number, $M_t$, 0.8; turbulence correlation length in direction transverse to flow, $\ell$, 1; eddy correlation length ratio, r, 1.